DETECTION OF STATOR WELDING FAULTS IN END-TURN WINDINGS OF AC MACHINES

By

Arslan Qaiser

A THESIS

Submitted to
Michigan State University
in partial fulfillment of the requirements
for the degree of

MASTER OF SCIENCE

Electrical Engineering

2013

ABSTRACT

DETECTION OF STATOR WELDING FAULTS IN END-TURN WINDINGS OF AC MACHINES

By

Arslan Qaiser

Electric machines are the powerhouse of industrial plants and processes and play a very important role in their efficient and safe running. These machines operate under electrical, mechanical and thermal stresses making them prone to failing. Faults in the stator windings, due to a weak welding joint is one of the types of failures that can propagate and eventually lead to severe consequences. Timely detection of these types of faults is therefore crucial to avoid any damage to the machine.

In this work, a framework has been put together for fault diagnosis, to detect and categorize a fault in the end turn windings of stators of PMAC and Induction motors. Feature extraction methods such as the Short Time Fourier Transform (STFT) and Wavelet Transform (WT) are implemented to extract the features by observing the energy densities. The features are categorized using classification methods like Nearest Neighbor Rule (NNR) and Linear Discriminant Analysis (LDA) to help classify the machine as either healthy or faulty, and identify the fault severity.

ACKNOWLEDGEMENTS

I would like to express my gratitude to my thesis advisor Dr. Elias Strangas for his continuous support and guidance. I would also like to thank Dr. Aviyente and Dr. Wierzba for their time in being a part of my committee. I would like to thank Dr. Aviyente in particular, for her guidance and insight provided throughout the course of this work.

I would like to extend my gratitude to my lab colleagues Carlos Nino, Andrew Babel, Jorge Rivera, Eduardo Montalvo and Reemon Haddad for their support. I owe special thanks to my parents, Qaiser Malik and Meena Qaiser, for all their encouragement and continuous support that made my studies possible.

TABLE OF CONTENTS

LIST OF TABLES

LIST OF FIGURES

Chapter 1

Introduction

The main objective of this thesis is to detect a welding fault in the end-turn windings of AC motors.

This document initially discusses literature that led to our approach to tackling the problem of fault analysis. The technique utilized are, time-frequency tools such as the Short Time Fourier Transform (STFT) and the Wavelet Transform (WT) to extract the features. Categorization methods such as the Nearest Neighbor Rule (NNR) and Linear Discriminant Analysis (LDA) are used to help detect, isolate and identify the fault. In the literature review, these methods are discussed in detail.

We consider the winding to be similar to a transmission line, where a pulse sent at a terminal will reflect back, and the reflections indicate the characteristics of the discontinuities. In the Background section, a simulation of the Transmission Line model is presented. It is used to understand the concept of reflectometry and give an idea of what to expect in the actual stator windings.

Problem Formulation and Proposed Solution section gives the similarity between a transmission line model and a machine model, since the two behave similarly under an impulse response.

The complete testing setup along with the equipment used and the testing method is discussed in the Experimental Setup section. Different fault severities and fault locations are considered for testing purposes and same experimental procedure is repeated to gather data. Resistors are used to simulate the fault severity and three different faults are created in the stator winding; fault at near the pulsing end, fault at center of the winding, and fault at quarter of a way into the winding.

The Results section discusses the various analysis methods used for detection and classification of faults. The STFT and WT are implemented and the energy spectrum of varying fault severity at different locations is compared to that of no fault (healthy case). Features are selected based on the dominant frequencies present in the signal for all times. NNR and LDA are applied to these selected features and the results are discussed.

Some suggestions for future work along with the conclusions are presented in the Conclusion section of this thesis.

Chapter 2

Background

2.1 Scope and Objective

The motivation of the approach is the concept of reflectometry applied to motors. A Stator winding behaves similarly to a transmission line when an impulse is applied. In a transmission line, the impulse reflects back from discontinuities and the pattern of the reflected pulses can be used to detect a fault. Many diagnostic methods have been proposed in the literature for different types of fault detection. Each one of these requires the knowledge of some key concepts and this chapter will look into some of these types of fault detection methods. These concepts involve the study of transmission line theory, time-frequency analysis methods, pattern classification methods and feature extraction methods.

This chapter is divided into several sections as follows: Section 2.2 gives a brief overview of the transmission line theory. Section 2.3 contains information about the methods that have been developed and applied to fault detection. Transformer Impulse Test is explained along with literature that applies this method. Section 2.4 gives details of the theoretical concepts that include feature extraction methods like Fourier Transform (FT), Short Time Fourier Transform

(STFT) and Wavelet Transform (WT). Section 2.5 discusses Classification Methods like Nearest Neighbor Rule (NNR) and Linear Discriminant Analysis (LDA).

2.2 Transmission Line Theory

A distributed parallel plate transmission line can be modeled as a lumped two-port network as shown in Figure 2.1. The values of the lumped parameters per unit length R, L, G, C can be calculated from the expressions given in Table 2.1.

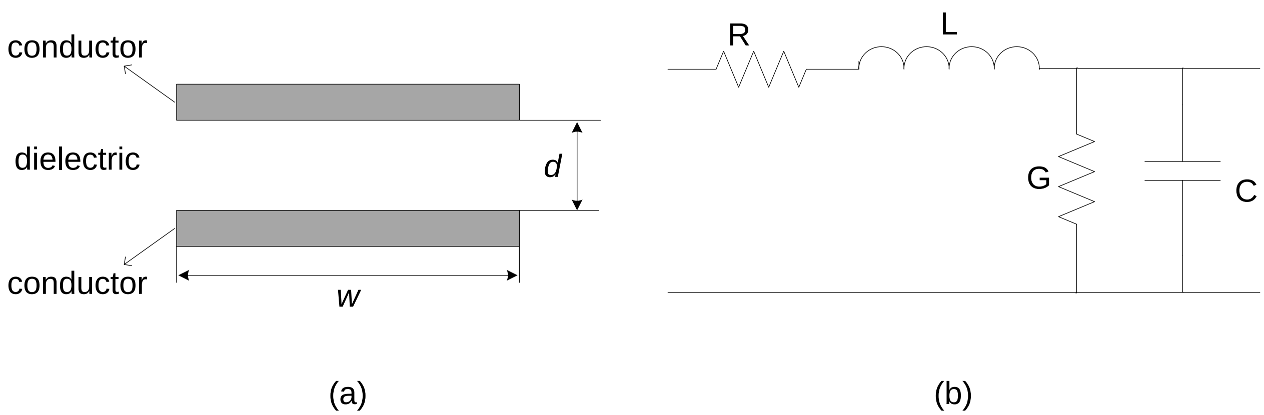

Figure 2.1: (a) Parallel plate transmission line in cross-section (b) Equivalent lumped model of a transmission line

Parameter	Expression	Units
R	$\frac{2}{w}\sqrt{\frac{\pi f \mu_C}{\sigma_C}}$	Ω/m
L	$\mu \frac{d}{w}$	H/m
G	$\sigma \frac{w}{d}$	S/m
C	$\epsilon \frac{w}{d}$	F/m

Table 2.1: Parameters of lumped transmission line

where w is the width of the plate, d is the separation between the bars, ϵ is the permittivity, σ is the conductivity and μ is the permeability of the dielectric material. σ_C and μ_C are the conductivity and permeability of the conductor.

The transmission line model can be analyzed in steady-state or transient conditions. Steady-state operation occurs when the transmission line is excited with a sinusoidal source of fixed amplitude and fixed frequency. Transient condition occurs when the transmission line is excited with a pulse.

The impedance of the transmission line is called the characteristic impedance, Z_0 which is fixed by the geometry of the conductors. From the transmission line model parameters stated above, the characteristic impedance can be calculated as

$$Z_0 = \sqrt{\frac{R + j\omega L}{G + j\omega C}} \tag{2.1}$$

When the transmission line is terminated with a load impedance equal to the characteristic impedance, then any input current or voltage distributions on the line are exactly the same as though the line had been extended to infinity. Under this condition, there are no reflections produced. However when the load impedance is different than the characteristic impedance, then the source will see reflected waves produced by the transmission line. Different values of load impedances produce different reflected waves. The study of welding faults will use this idea by observing a change in the reflected waveform with the change of load impedance. The reflected waveform will be different for different resistance values.

As an example, consider a transmission line of length l connected to a source of impedance Z_g and a resistive load Z_l. Refer to Figure 2.2.

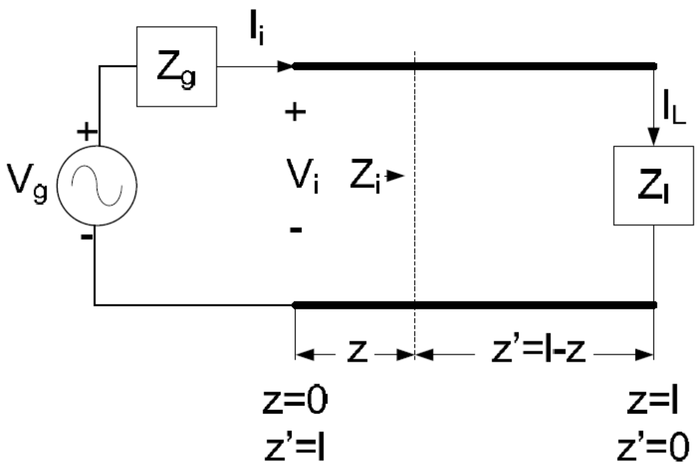

Figure 2.2: Transmission line example terminated with load impedance

The voltage and current in the transmission line are given as:

$$V(z') = \frac{I_L}{2}(Z_L + Z_0)e^{-\gamma z'}\left[1 + \Gamma e^{-2\gamma z'}\right] \tag{2.2}$$

$$I(z') = \frac{I_L}{2Z_0}(Z_L + Z_0)e^{\gamma l}\left[1 + \Gamma e^{-2\gamma l}\right] \tag{2.3}$$

Where

$$\gamma = \alpha + j\beta = \sqrt{(R + j\omega L)(G + j\omega C)} \tag{2.4}$$

$$I_L = \frac{V_L}{Z_L} \tag{2.5}$$

$$\Gamma = \frac{Z_L - Z_0}{Z_L + Z_0} \tag{2.6}$$

I_L and V_L are the current and voltage measured at the load, Z_L. $e^{\gamma l}$ and $e^{-\gamma l}$ represent the incident and reflected wave component respectively. Γ is the reflection coefficient and the amplitude of reflected wave depends on the difference between Z_L and Z_0.

In Time Domain Reflectometry (TDR) test, the transmission line is excited by a narrow pulse. A reflected pulse is generated due to the unmatched impedance between the line and the load. In case of a faulty system, a second reflection will be produced from the discontinuity and travels back to the source. These incident and reflected waves are plotted against time, and the time difference between these pulses indicates the location of the fault.

2.2.1 Simulation

In this section, simulation results from the transmission line model are shown. A simple model of a healthy transmission line is shown in Figure 2.3. The four segments of the line are identical and connected together to form the transmission line. Each of these segments is made up of the lumped model given in Figure 2.1. The termination is variable impedance set to 100 Ω. The parameters of the transmission line are defined as follows:

Parameters: R = 0 Ω

L = 0.0063 nH

C = 0.0063 pF

The characteristic impedance is calculated using, $Z_0 = \sqrt{L/C} = 31.6228$ Ω. The termination is set to 1 KΩ in order to have mis-matched impedance because in case of matched impedance, there will be no reflection. The source impedance Z_S is set equal to Z_0 in order to have no reflection coming from the source end. Hence the pulse reflects only at the termination as seen in the plot below.

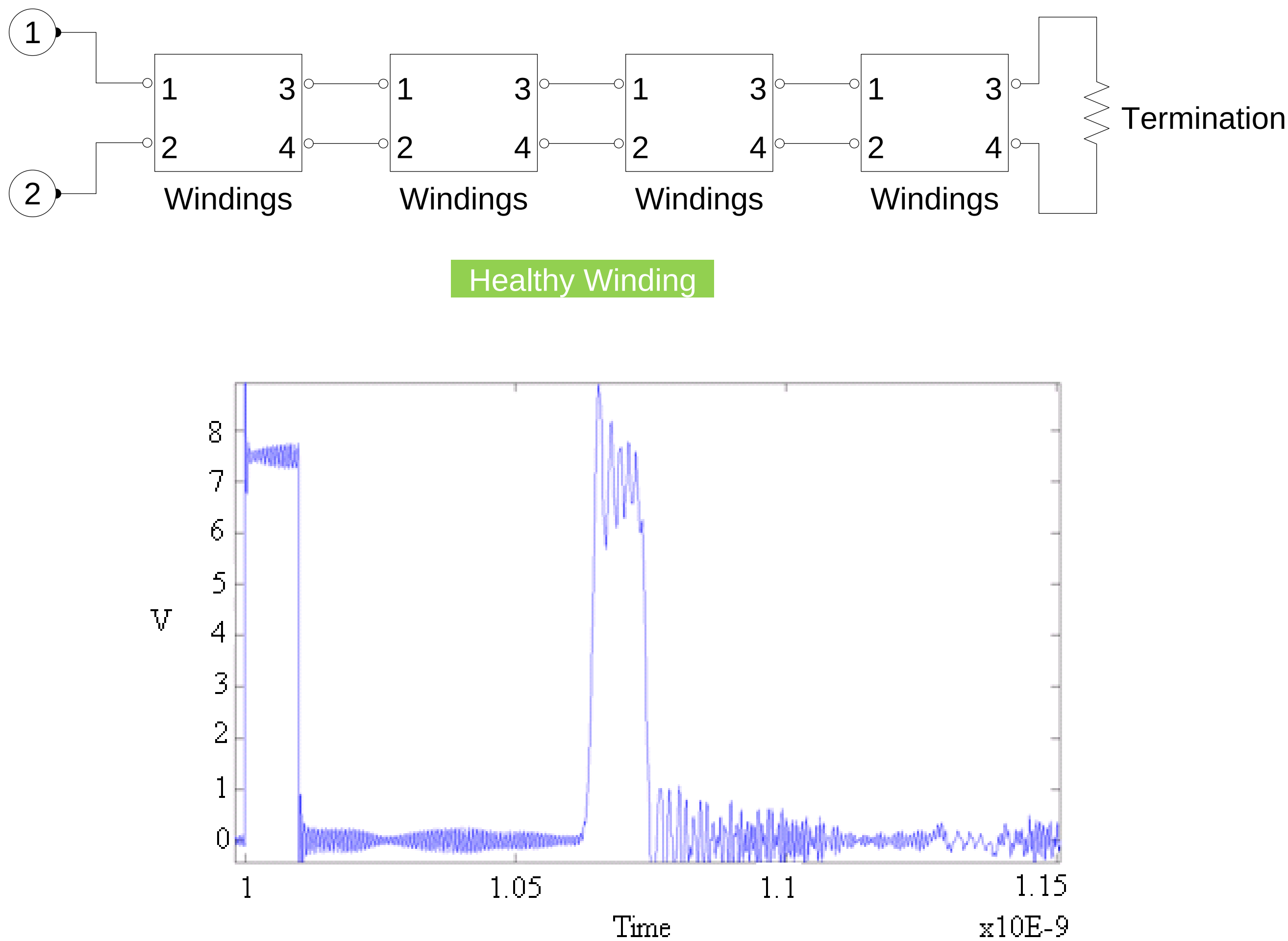

Figure 2.3: Model of healthy line (“For interpretation of the references to color in this and all other figures, the reader is referrred to the electronic version of this thesis.”)

In the first case, a fault exists in the middle of the line. The fault used here is a series resistance of 50 Ω. When a pulse is sent into the transmission line, it encounters two discontinuities: the termination and the fault. We would expect to see two reflections, one from each discontinuity. The simulation result in Figure 2.4 shows exactly this. The reflection from the fault is located at the center of initial pulse and the reflection from the termination.

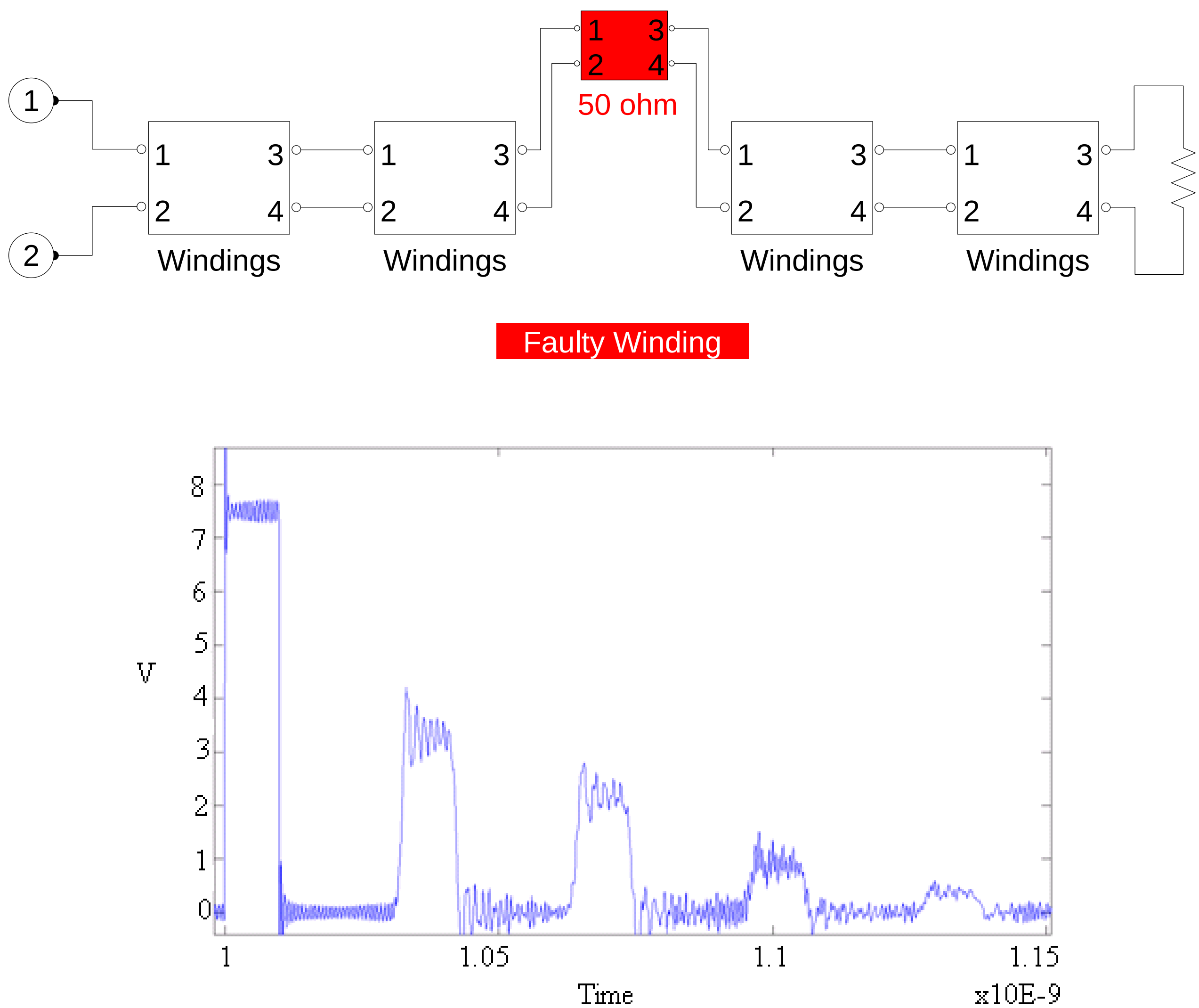

Figure 2.4: Model of faulty line (fault at center)

Next we consider a case in which the fault location is closer to the input end of the transmission line as seen in Figure 2.5. When a pulse is sent into the transmission line, it will again encounter the same two discontinuities. We can see from the output plot that the reflection due to termination is same as Figure 2.4. However, the reflection due to the fault is shifted and corresponds to the shift of the fault in the line. This confirms that the reflection pattern changes with the location of the fault.

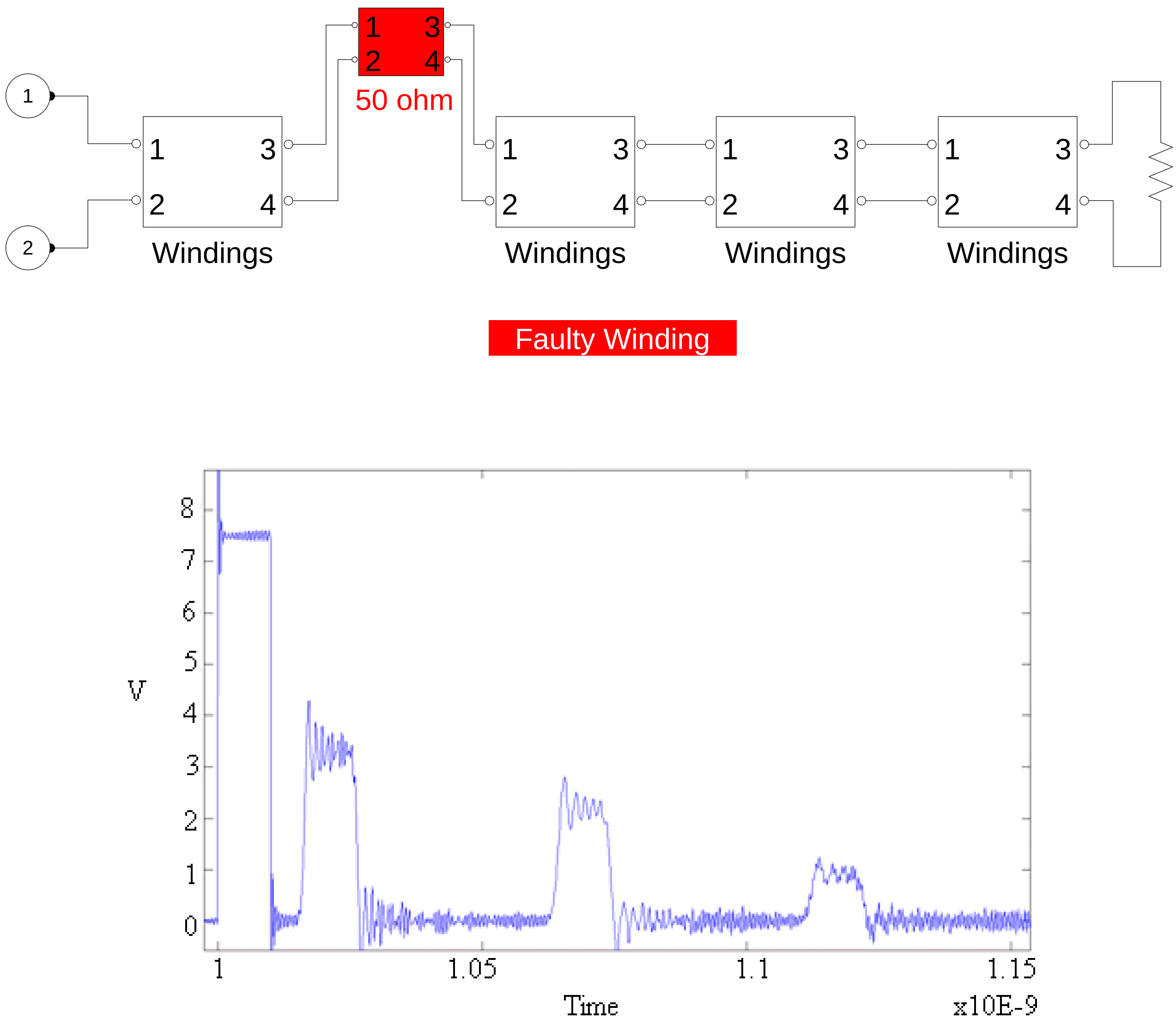

Figure 2.5: Model of faulty (fault at beginning)

The proposed solution to the problem of detecting faults in a stator winding is to use the concept of reflectometry and apply that to the stator winding. The reflections observed in a transmission line can be used to determine the termination of a transmission line and also if there are any discontinuities in it. We extend the case of the stator windings to observe the reflections after sending an input pulse and aim to detect a fault from these reflections.

2.3 Literature Review

In this section, a literature review is presented for impulse test in motors and transformers and fault detection tests in transmission lines. These methods are different from the proposed method in this work, but the fault detection methods share similarities. Two types of pulse waveforms are typically used for fault detection, low rise time high voltage pulse and high frequency low energy pulse. The low rise time high voltage pulse is a standard 1.2x50 μs used for impulse test in transformer/motor.

2.3.1 Transformer Impulse Test

The voltage waveform that is used in transformer impulse test is called a full-wave lightning impulse [1]. This is a wave that has a rise time of 1.2 μs and decays to half of the peak value in 50 μs, hence the name 1.2x50 μs wave. The waveform shape is shown in Figure 2.6 below.

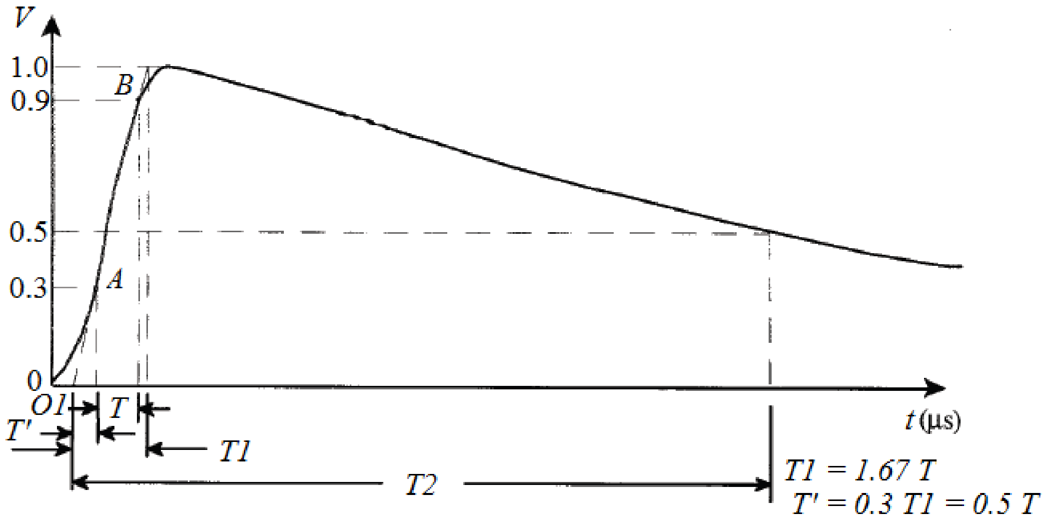

Figure 2.6: Transformer Impulse Test waveform

The time characteristics of the full-wave lightning impulse are explained as follows:

Virtual Front Time (T1)

The virtual front time (T1) of a lightning impulse is defined as the time it takes for the impulse to reach between 30% and 90% of its peak value, which corresponds to points A and B in Figure 2.6

Virtual Origin (O1)

The virtual origin (O1) of a lightning impulse is the instant right before the time corresponding to point A given by 0.3 T1. This is obtained by drawing a straight line that joins points A and B and intersects with the time axis.

Virtual time to half value (T2)

The virtual time to half value is the time from the virtual origin to the instant on the tail when the voltage reaches half of the peak value.

A typical impulse test configuration is shown in Figure 2.7 below, where the detailed connections are shown in the following Figure 2.8 [2].

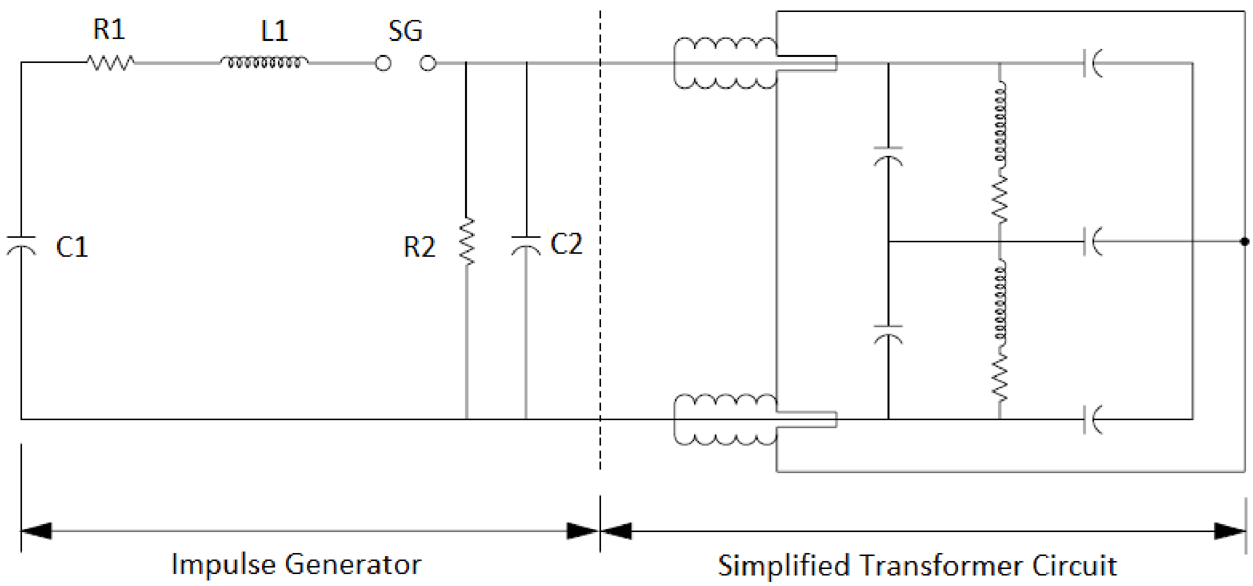

Figure 2.7: Typical lightning impulse circuit

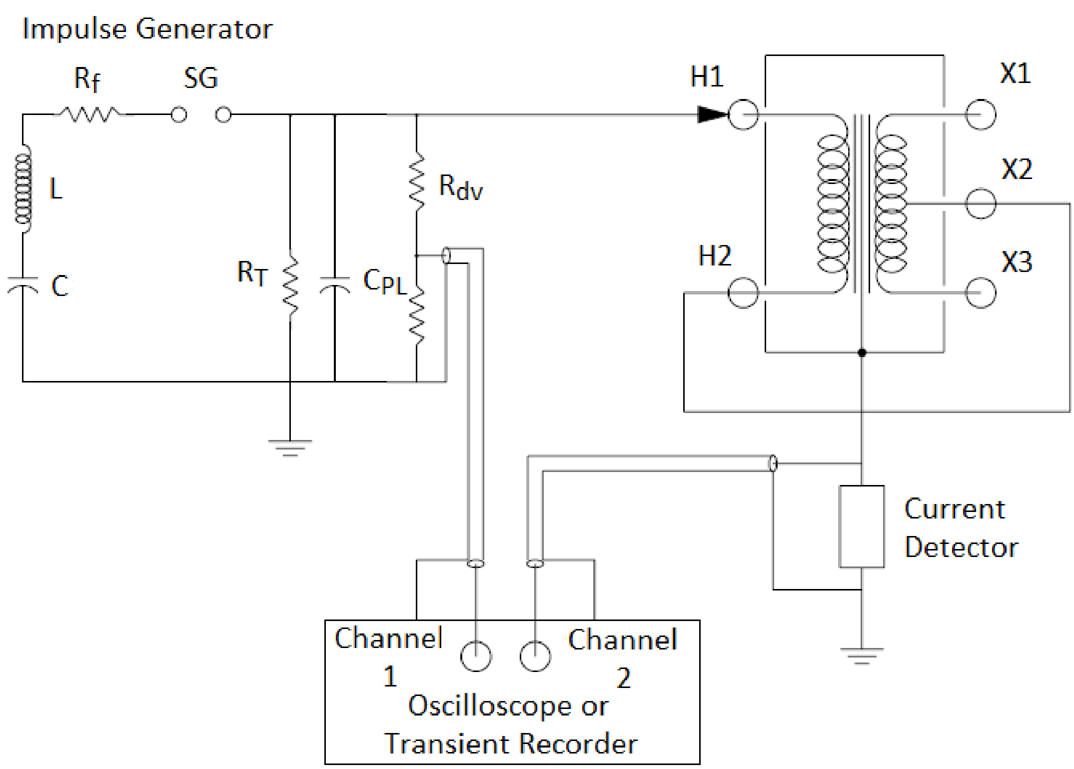

Figure 2.8: Typical transformer connection for routine impulse testing

Fault detection schemes based on these impulse tests are developed and usually involve either measuring the input voltage or the neutral current and comparing it with those of non faulty cases. There are two types of neutral current detection methods, (a) the ground-current method and (b) the neutral-impedance method. It is the relative values of resistance and capacitance used in the shunts or connected across the output of the wide-band current transformers that qualify them as either of the detection methods. The ground current method uses lower values of resistances and capacitances that allows for lower time constant and higher bandwidth, rather than high value components used in the neutral impedance method. The following required characteristics of the measurement system were taken from the standard "IEEE Std C57.138-1998".

- The shunt elements, R and C are chosen to provide a peak voltage of 700 to 1000 V. These values can vary depending on the design of the transformer.

- The value of capacitor typically controls the peak voltage. It is used to limit the current during faults, thus the capacitor should be selected to produce good resolution in the oscilloscope under any conditions. Typical values of capacitance range from 0.05 μF to 2.0 μF.
- The value of resistor is chosen to achieve a voltage decay to half value in the 50 to 2000 microsecond range.
- The current transformer (CT) should be a precision wide-band type, with a rise-time of 20 nanoseconds or less and a droop of less than 0.1% per microsecond. Rise-time is a measure of the CTs ability to respond to the high frequency components of current and droop is a measure of the response to the low frequency components.

Several hardware configurations have been described in the standard “IEEE Std C57.138-1998” to automatically detect a fault, but the dependence on the tested transformer makes them irrelevant to the analysis presented in this work.

2.3.2 Previous Work

Several techniques have been developed for motors, transformers and transmission lines to detect faults in welding and insulation of the winding. Some of these are mentioned below:

- Mehdi *et al.* [3] discusses incipient faults in the windings of transformers that result due to the insulation breakdown during an impulse test. These faults are hard to detect since they are low amplitude and occur as transients. The ‘Arc Discharge method’ is discussed which uses the Transformer winding model as a basis. The model consists of a double disc where each disc represents a series resistance, self inductance, shunt resistance, series capacitance and ground capacitance and the mutual inductance between the discs.

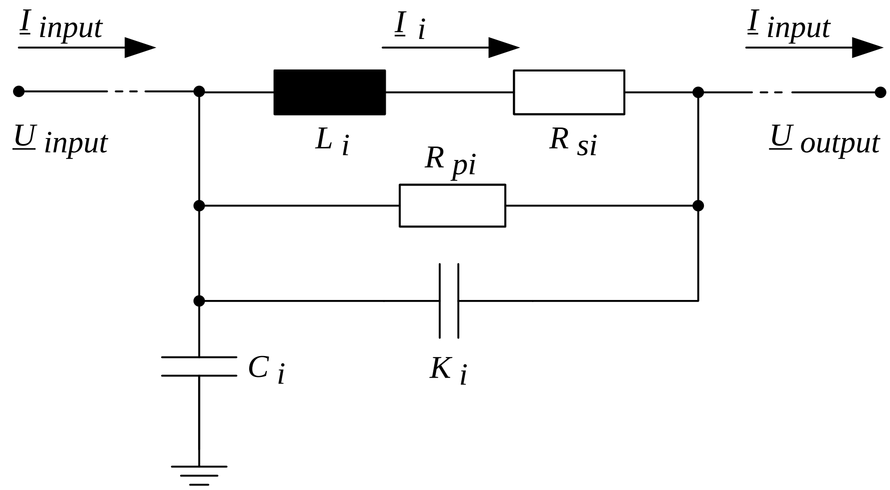

Symbol	Description
R_{si}	Series resistance
L_i	Self inductance
R_{pi}	Shunt resistance
K_i	Series capacitance
C_i	Ground capacitance

Figure 2.9: Detailed transformer model

Since the arcing occurs between the discs of the transformer model, Mayr Equation is used to explain this phenomenon [4].

$$\frac{1}{R}\frac{dR}{dt} = \frac{1}{\tau}\left(1 - \frac{v \times i}{P_0}\right) \tag{2.7}$$

where R is the arc resistance, v is the arc voltage, i is the arc current, P_0 is the momentary constant power loss and τ is the time constant. Mayr Equation can be written in terms of the arc conductance, g

$$g + \tau\left(\frac{dg}{dt}\right) = \frac{i^2}{P_0} \tag{2.8}$$

In transformers, the gap between the two discs of the winding is typically low, so the power losses in the arc column are low. Also the arc between winding discs is a fast decaying and low energy phenomenon, thus the term i^2/P_0can be considered a constant. The variation of arc conductance is represented by

$$\begin{cases} g + \tau\left(\frac{dg}{dt}\right) = g_{st} \ , & t \geq t_{arc} \\ g = 0 \ , & t < t_{arc} \end{cases} \tag{2.9}$$

where g_{st} is a conductance constant and t_{arc} is the start time of the ignition phase. The arcing between the discs is represented by a non-linear time varying conductance, $g_{arc}(t)$, that increases as an impulse voltage is applied.

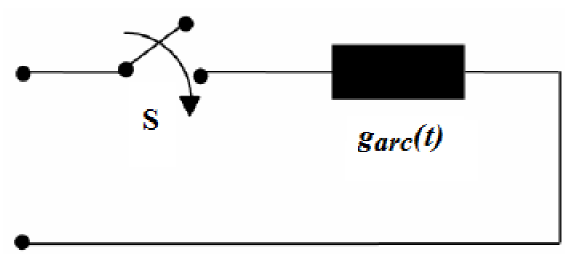

Figure 2.10: Arc discharge model

A lightning impulse, as used in transformer impulse tests, is applied to the input terminal and the input current in the case of arc discharge occurrence is recorded as shown in Figure 2.11 below. The arc discharge is most likely to happen at the peak of the input voltage. The fast changes in the input current can be attributed to the arc discharging phenomenon.

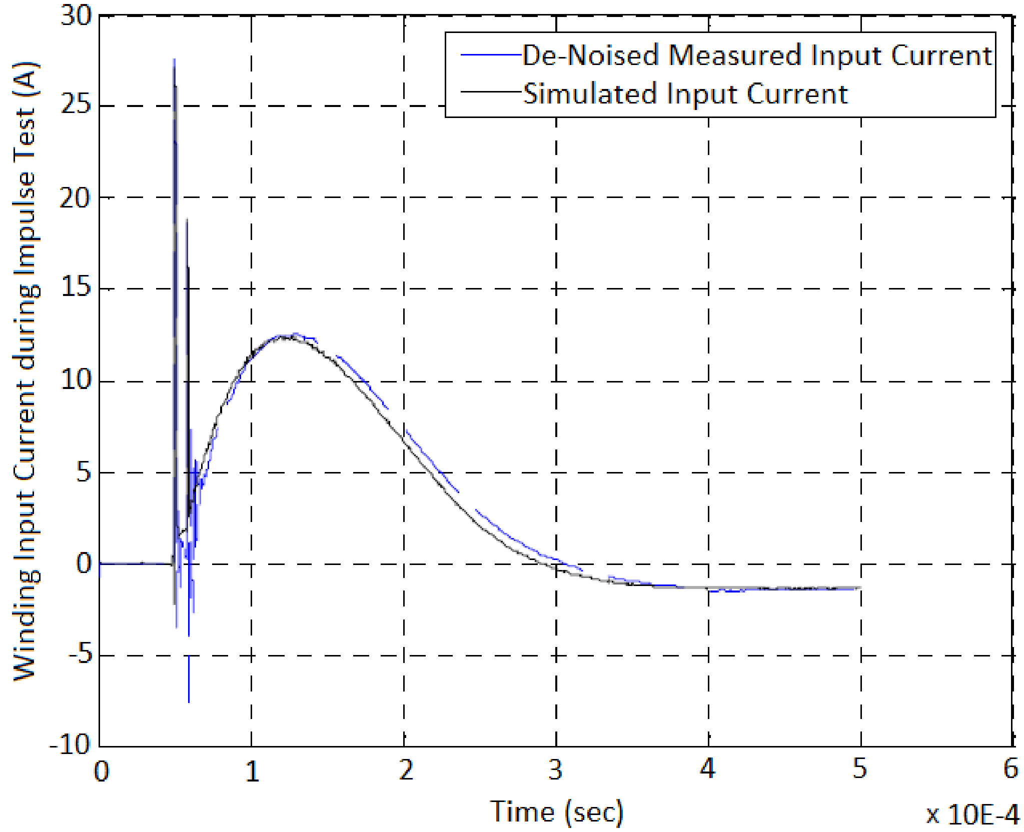

De-Noised Measured Input Current
Simulated Input Current
Winding Input Current during Impulse Test (A)
Time (sec)
x 10E-4
30
25
20
15
10
5
0
-5
-10
0
1
2
3
4
5
6

(a)

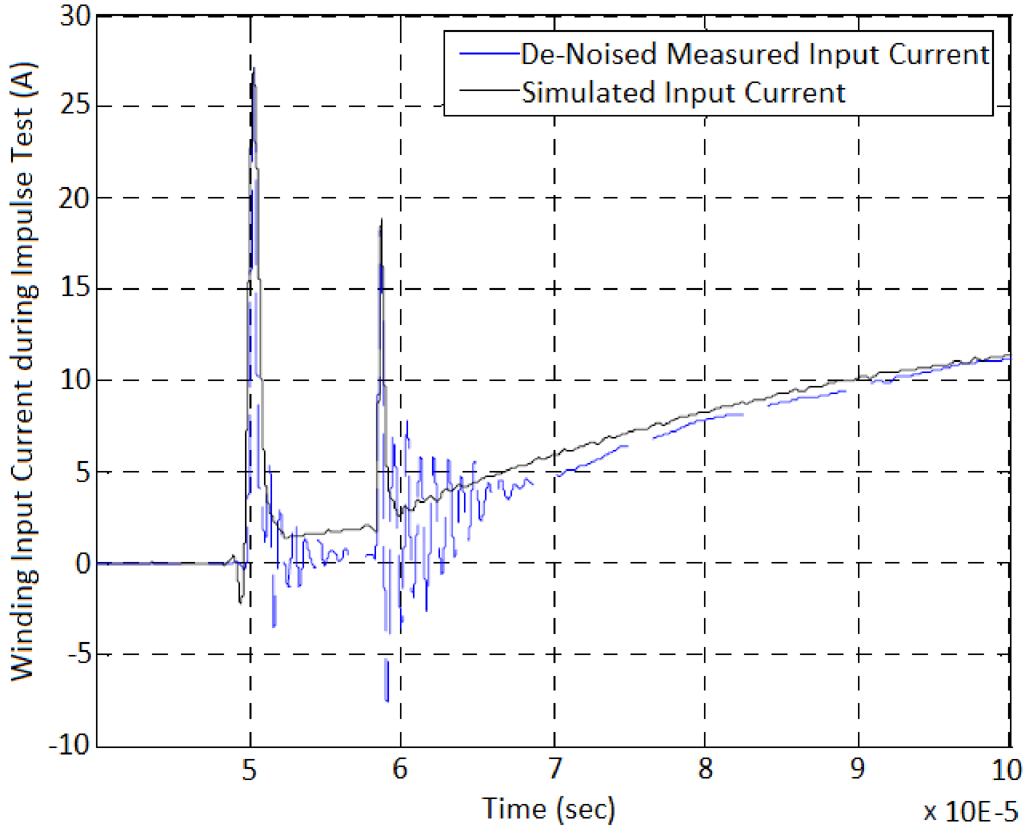

(b)

Figure 2.11: Simulated and measured disc-disc arc discharge, (a) full scale (b) zoomed

- Essam *et al.* [5], [6] proposed a time-frequency analysis method to improve the fault detection in transformers under the impulse test. Frequency Response Analysis (FRA) method has been used widely to obtain transfer functions by using the input current and output voltages. Fast Fourier Transform was traditionally used as the standard technique in FRA, but the sensitivity of the fault detection can be improved by using Short Time Fourier Transform (STFT) for the evaluation of impulse tests on transformers. The FRA can be categorized in different frequency ranges: low, medium and high frequencies responses. The low and high frequency responses are significant in FRA for inter-turn faults in transformers. Various diagnostic criteria like the absolute sum of logarithmic error (ASLE) and sum squared ratio error can be used to determine the fault in transformer.

Relative changes in amplitude and resonant frequency location can help distinguish the various types of failures and provide an indication for test repeatability. The relative change in amplitude (DA) and relative change in resonant frequency location (Df) are computed as:

$$DA = \frac{A_i - A_n}{A_n} \times 100 \tag{2.10}$$

$$Df = \frac{f_i - f_n}{f_n} \times 100 \tag{2.11}$$

where A_n and f_n are the magnitude and resonant frequency location for the fingerprint (normal conditions). A_i and f_i are the magnitude and resonant frequency location for all other simulated conditions. The use of STFT gives another useful factor, relative change in time (Dt)

$$Dt = \frac{t_i - t_n}{t_n} \times 100 \tag{2.12}$$

where t_n is the time at which the resonant frequency of a fingerprint occurs, and t_i is the time at which resonant frequency occurs for all other simulated conditions.

The Short Time Fourier Transform (STFT) is used for time-frequency analysis. The STFT is simply a windowed FT that is applied for the complete duration of the time. Each windowed segment gives a time-frequency representation of the signal. The transfer function based on the STFT is the ratio of the input current (I_1) to the output voltage (V_2) called the trans-admittance transfer function. The STFT for each quantity is computed and the resultant transfer function is given as

$$TF = \frac{STFT(I_1)}{STFT(V_2)} \tag{2.13}$$

The transformer under test had the following specifications: 25 kVA, 7200/12470Y, 120/240, 60 Hz. The impulse wave shape is selected from the routine impulse testing of transformers to be the full-wave lighting impulse 1.2x50 μs. The test setup is shown in Figure 2.12 below with four types of faults.

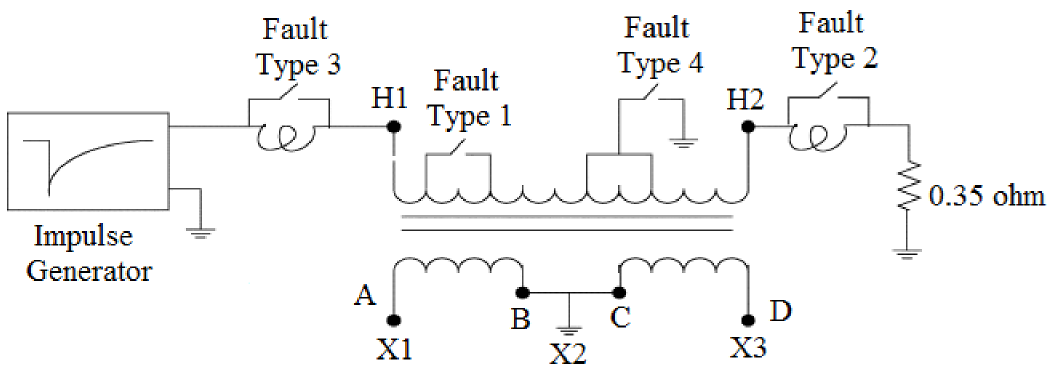

Figure 2.12: Four kinds of faults made to the transformer

When the transformer windings are excited by an impulse, the voltage and current waveforms are non-stationary signals, i.e. signals that are aperiodic in nature. The primary current and secondary voltage signals were recorded using high-resolution oscilloscope for different cases of faults as shown in Figure 2.12 above. In time domain, some difference can be seen when comparing the current and voltage waveforms, but it is hard to tell apart a fault from healthy case, Figure 2.13. Time-frequency analysis such as STFT is used to identify certain frequencies that may be affected more due to the presence of a fault. Figure 2.14 shows the 3D STFT spectrograms.

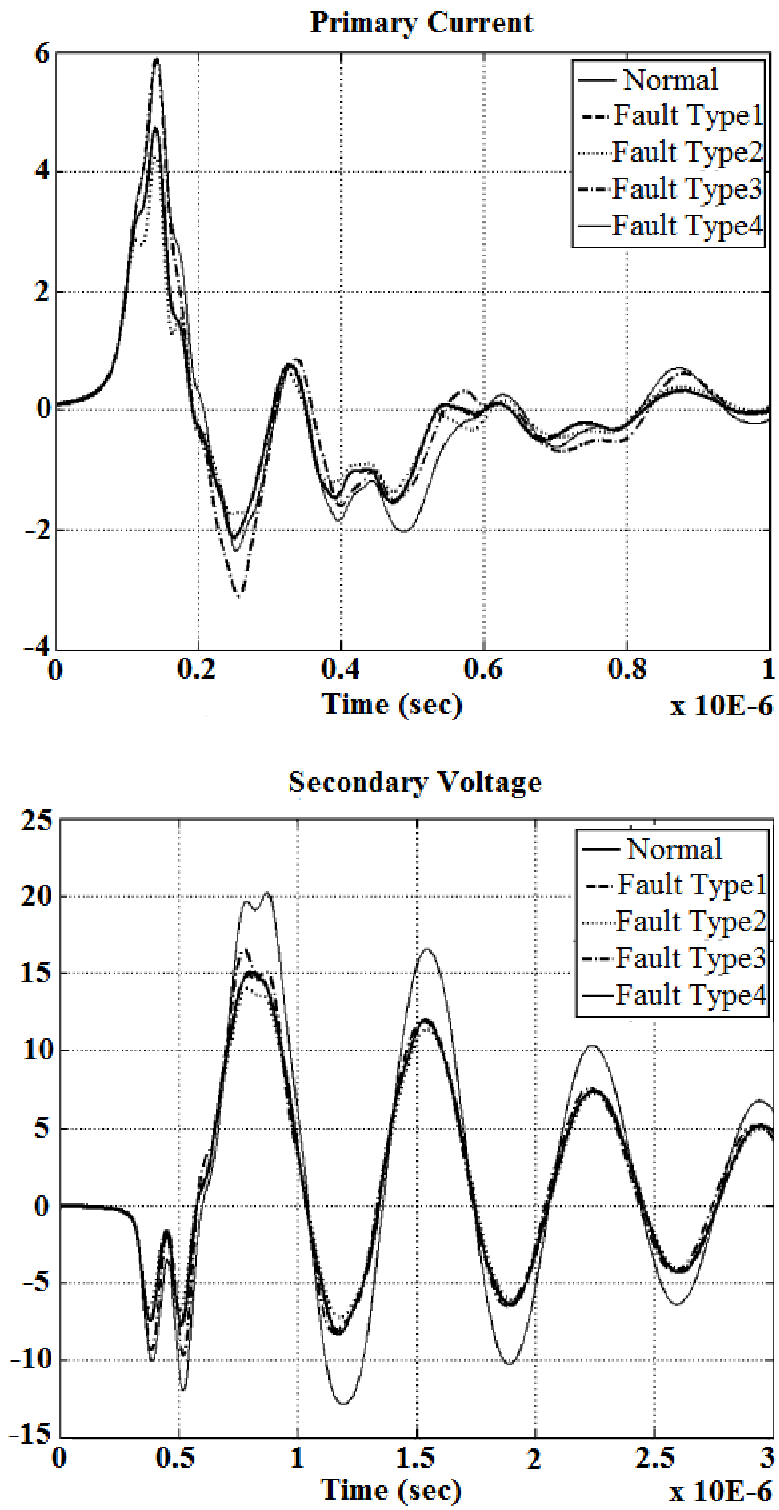

Figure 2.13: Time domain representation

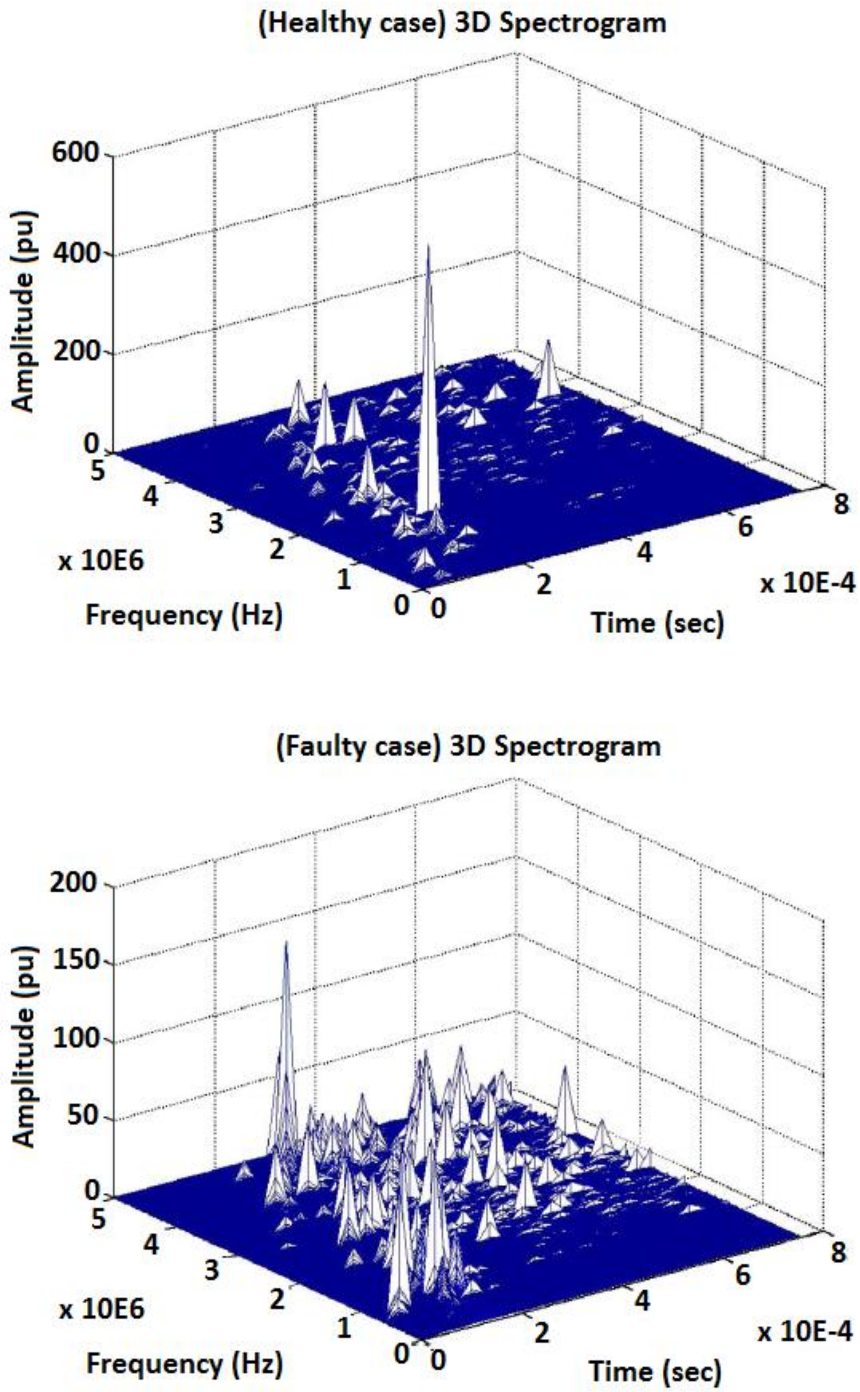

Figure 2.14: Spectrograms of (a) healthy , (b) faulty cases

- Purkait *et al.* [7] used wavelet analysis to detect faults in transformers when an impulse test is applied. Winding current waveforms are used for wavelet analysis where the pattern of the currents changes depending on the type of fault, and where it is located. Clustering analysis is used to classify the transformer faults. Electromagnetic Transient Program (EMTP) based models of transformers are used for this detection method. Known faults in the transformer winding were created which can be of two types: series or shunt fault. Series faults are characterized by insulation failures between the turns of the winding and a shunt fault is characterized by the insulation failure between the winding and ground. Different faults were created for the entire length of the winding and the time domain current waveforms were analyzed for each fault type. Wavelet analysis using the Morlet mother wavelet was applied and a 3D representation of the wavelet coefficients with respect to translation (time) and scale was obtained as shown in Figure 2.15 below.

Selected parameters were chosen from these 3D wavelet plots for classification purposes. Three parameters of interest are the predominant frequency component, its corresponding time of occurrence and the corresponding wavelet coefficient. The predominant frequency component is the one which has the highest value of coefficient for all times.

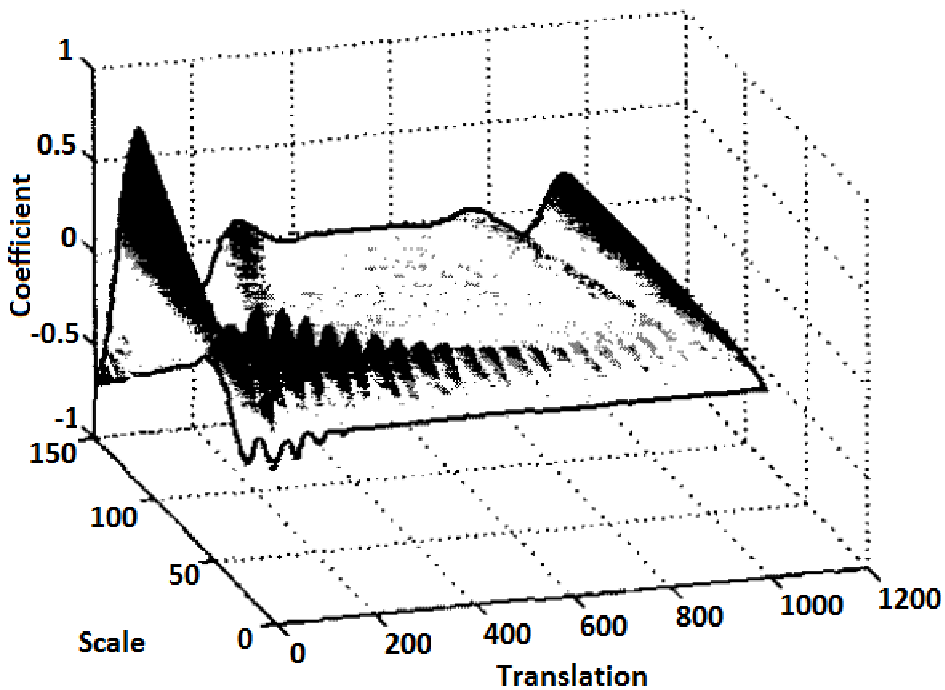

Figure 2.15: 3D surface plot of time domain current waveform

These same three parameters are selected for the different types of faults created in the transformer winding and by using clustering, a unique pattern can be seen for the same types of faults. Each fault type has its own signature that makes it different in terms of its predominant frequency and the corresponding time and wavelet coefficient. The result of clustering can be seen in Figure 2.16 below, where a 2D plot of scales vs. wavelet coefficient is shown. Separate clusters are formed for each type of fault (shown for only series fault), and thus using wavelet analysis, impulse faults in transformers can be detected.

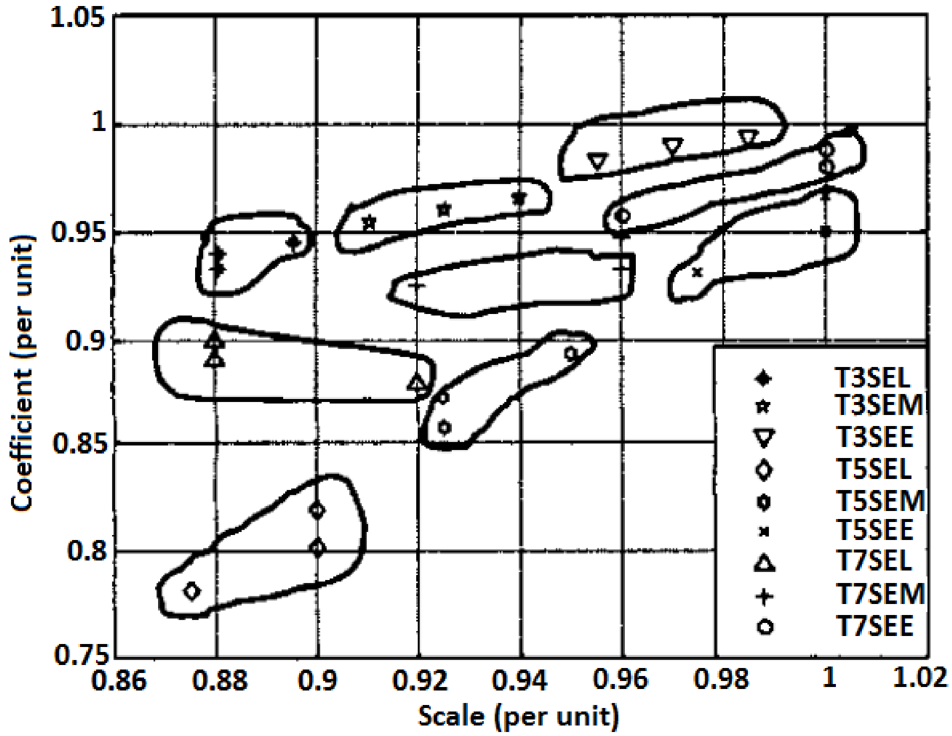

Figure 2.16: 2D plot of scales vs wavelet coefficients for series faults

2.4 Theoretical Background – Time-frequency Analysis

Time domain analysis is used primarily for steady-state operation. It is insufficient to monitor small changes in transients. Frequency domain analysis like the Fast Fourier Transform (FFT) provides frequency components in a signal but does not contain the time information on when these frequency components occur. Time-frequency analysis is inherently used to detect small changes in transients. Techniques like the Short Time Fourier Transform (STFT) and Wavelet Transform (WT) provide a way to analyze both the time and frequency information simultaneously. This section provides a detailed theoretical background on both of these time-frequency analysis methods.

2.4.1 Short Time Fourier Transform

The Fourier Transform of a signal $x(t)$ involves decomposing it into its constituent frequencies that can be written as a sum of sines and cosines. Mathematically it can be written as:

$$X(\omega) = \mathcal{F}[x(t)] = \int_{-\infty}^{\infty} x(t)e^{-j\omega t}dt \qquad (2.14)$$

The Fourier transform is valid for stationary signals only. However most signals are non-stationary and the Fourier transform cannot be applied. For such cases, we make use of the Short Time Fourier Transform. It is defined as the Fourier Transform of a windowed section of the signal, $x(t)$. Figure 2.17 shows the concept of 'windowing' a signal, which means to take a small segment of the signal, so that the signal is almost stationary in that window frame, and then applying the usual Fourier Transform to the windowed part. The window then slides across the whole signal, each time computing the Fourier Transform. In the end all the individual windowed Fourier Transform are summed together to give the Short Time Fourier Transform. The tiling for the STFT is shown in Figure 2.18 below.

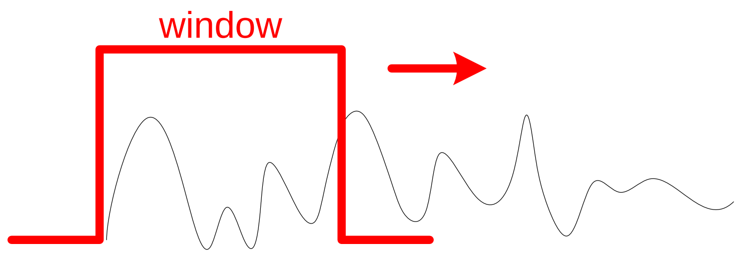

Figure 2.17: FT of a windowed section of signal

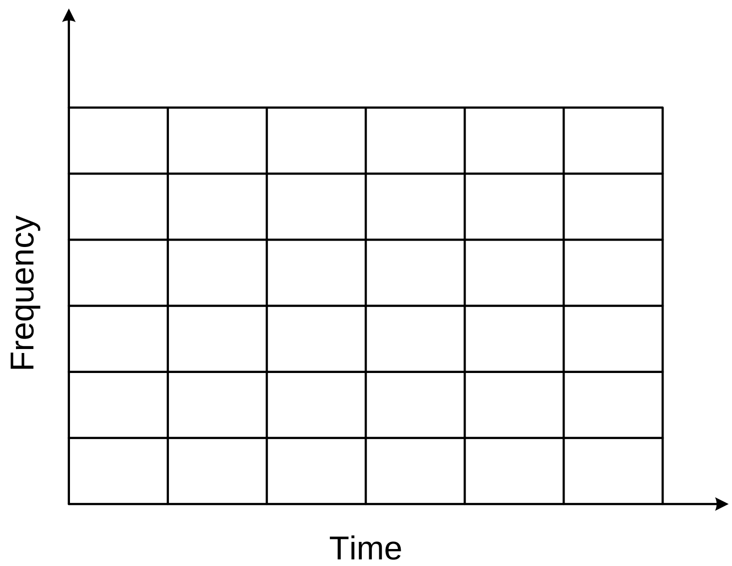

Figure 2.18: STFT time-frequency tiling

Mathematically the short time Fourier Transform is defined as follows:

$$X(\omega, t') = \int_{-\infty}^{\infty} x(t)w(t-t')e^{-j\omega t}dt \tag{2.15}$$

where, ω = frequency to be analyzed,

$x(t)$ = time signal

$w(t)$ = type of window

There are two key concepts in the STFT

1. Time resolution
2. Frequency resolution

In order to explain these concepts, consider a window *w(n)* of length N, whose Fourier Transform is given by the sinc function, *W(f)* given below.

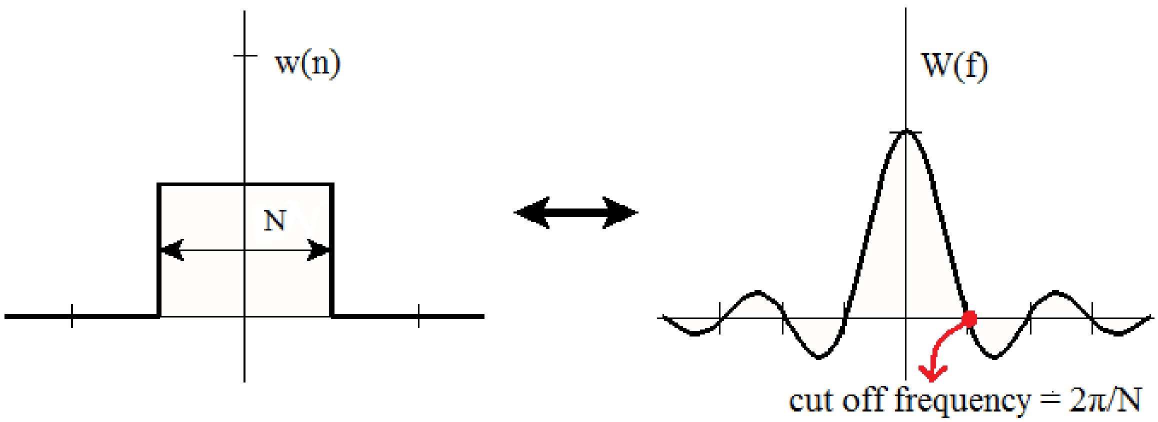

Figure 2.19: Rectangular window (left), Sinc function (right)

The sinc function has a cut-off frequency given by $\frac{2\pi}{N}$. Now consider a signal *x(t)* to which the window *w(n)* will be applied.

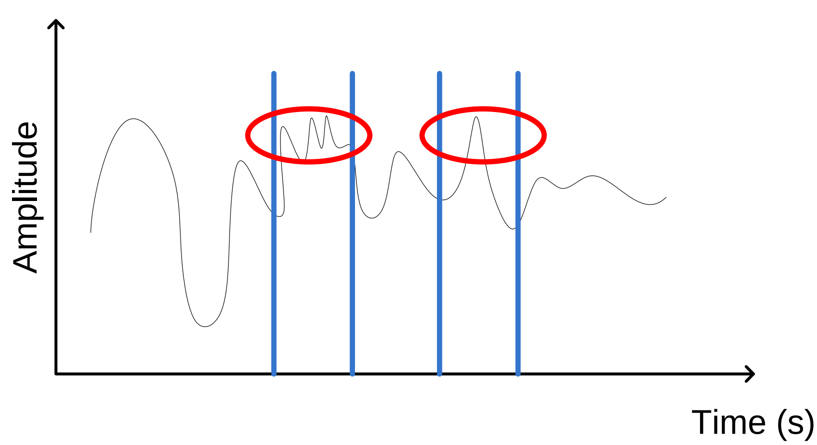

Figure 2.20: Signal *x(t)*

In order to achieve good temporal resolution, a short window length is required. This means that for small N, high frequency transients can be localized (as shown in Figure 2.20). The red circles indicate high frequency transients and the window length needs to be small enough to be able to detect these transients. However, by making N small, the cut-off frequency of the sinc function (also called a Low Pass Filter – LPF) increases. This results in a LPF with a large cut-off frequency. This means that the LPF will not be able to effectively reject all the low frequency content. We can say that if the window length N is small, the ability to distinguish between two adjacent frequency components goes down. Consider the other case when a longer window length N is chosen. This implies that the LPF will have a sharp cut-off frequency and the high frequency will be rejected more effectively, thus, giving good frequency resolution. However, a longer window also implies that high frequency transients will not be localized, resulting in bad temporal resolution. We can conclude from this discussion that both temporal and frequency resolution cannot be improved simultaneously.

There are certain limitations to the use of the STFT. The most important one is that the 'Time-Frequency' resolution is fixed, since choosing a fixed window length N fixes the bandwidth of the LPF. The time-bandwidth product is given by

$$\Delta t \cdot \Delta f \geq K,$$

where *K* is some constant

$$\Rightarrow \; \Delta t \propto \frac{1}{\Delta f}$$

This implies that good time resolution can only be achieved at the cost of poor frequency resolution and vice versa.

2.4.2 Wavelet Transform

Wavelet analysis is also used for non-stationary signals. First some notation will be defined to understand Wavelets better. $L^p(\mathbf{R})$ is the Hilbert space for measurable integrable functions f(x)

$$\int_{-\infty}^{+\infty} |f(x)|^P \, du < +\infty \tag{2.16}$$

$L^2(\mathbf{R})$ is the Hilbert space for square integrable functions, where $f(x) \in L^2(\boldsymbol{R})$. (2.17) is a subset of (2.16):

$$\int_{-\infty}^{+\infty} |f(x)|^2 \, du < +\infty \tag{2.17}$$

Consider a vector space V where a set of linearly independent functions that span V is called a basis. That is, any function V can be written as a linear combination of the basis functions. This can be shown by the linear decomposition (2.18) where f(t) represents any function in the space V, $\psi_l(t)$ are the basis functions, and a_l are the scaling coefficients,

$$f(t) = \sum_{l} a_l \, \psi_l(t) \tag{2.18}$$

A wavelet system is defined as a set of scaling functions and wavelet functions and is a basis for the set of functions belonging to $L^2(\mathbf{R})$ space. It is important to note that the scaling function, wavelet function and the basis function all have finite energy, which gives wavelets the ability to localize in time and frequency [8]. There are two types of wavelet transforms, namely Continuous Wavelet Transform (CWT) and the Discrete Wavelet Transform (DWT)

To define the CWT, consider a function $\psi(x)$ which is said to be a wavelet if and only if its Fourier Transform $\hat{\psi}(x)$ satisfies

$$\int_0^{+\infty} \frac{\left|\hat{\psi}(\omega)\right|^2}{\omega} d\omega = \int_{-\infty}^{0} \frac{\left|\hat{\psi}(\omega)\right|^2}{\omega} d\omega = C_\psi < +\infty \tag{2.19}$$

$$\int_{-\infty}^{+\infty} \psi(u)\, du = 0 \tag{2.20}$$

The continuous wavelet transform of a function is denoted by W*f(s,x)*, a function of both scale and position x (or time t). So the continuous wavelet transform is defined for the scale-space or scale-time plane. A wavelet function for a specific scale s can be defined as

$$\psi_S(x) = \left(\frac{1}{s}\right) \psi \left(\frac{x}{s}\right) \tag{2.21}$$

and the continuous wavelet transform of a function *f(x)* at scale s is given by

$$Wf(s,x) \triangleq f * \psi_S(x) \tag{2.22}$$

Note that at scale = 1, $\psi_S(x)$ is often referred to as the mother wavelet.

The discrete wavelet transform can be defined using the idea of multiresolution by starting with the scaling function and defining the wavelet function in terms of it [8]. A basic one-dimensional scaling function can be designed to translate a function in time (2.23) where **Z** is the set of all integers.

$$\varphi_k(t) = \varphi(t-k) \quad k \in \boldsymbol{Z} \quad \varphi \in L^2 \tag{2.23}$$

Wavelet systems are two-dimensional, so a scaling function $\varphi_{j,k}(t)$ that both scales and translates a function $\varphi(t)$

$$\varphi_{j,k}(t) = 2^{j/2}\varphi\left(2^j\left(t - 2^{-j}k\right)\right) \quad j,k \in \boldsymbol{Z} \quad \varphi \in L^2 \tag{2.24}$$

Where j is the log_2 of the scale and $2^{-j}k$ represents the translation in time. A subspace of the $L^2(\mathbf{R})$ functions can be defined as the scaling function space $\mathcal{V}$. $\varphi_{j,k}(t)$ spans the space $\mathcal{V}_j$, meaning that any function in $\mathcal{V}_j$ can be represented by a linear combination of functions of the form $\varphi_{j,k}(t)$ [8].

When discussing scaling functions in terms of multiresolution analysis, the relationship between the span of scaling functions with different indices can be seen in (2.25-2.26)

$$\cdots \subset V_{-2} \subset V_{-1} \subset V_0 \subset V_1 \subset V_2 \subset \cdots \subset L^2 \tag{2.25}$$

$$V_{-\infty} = \{0\}, \quad V_{\infty} = L^2 \tag{2.26}$$

Another subspace of $L^2(\mathbf{R})$ functions is the wavelet vector space $\mathcal{W}$. A wavelet spans the space $\mathcal{W}_j$, which represents the difference between two scaling function spaces, $\mathcal{V}_j$ and $\mathcal{V}_{j+1}$. It can be seen that (2.27) extends to (2.28)

$$\mathcal{V}_1 = \mathcal{V}_0 \oplus \mathcal{W}_0 \tag{2.27}$$

$$L^2 = \mathcal{V}_0 \oplus \mathcal{W}_0 \oplus \mathcal{W}_1 \oplus \cdots \tag{2.28}$$

The relationship between the scaling function and the wavelet vector space is illustrated in Figure 2.21.

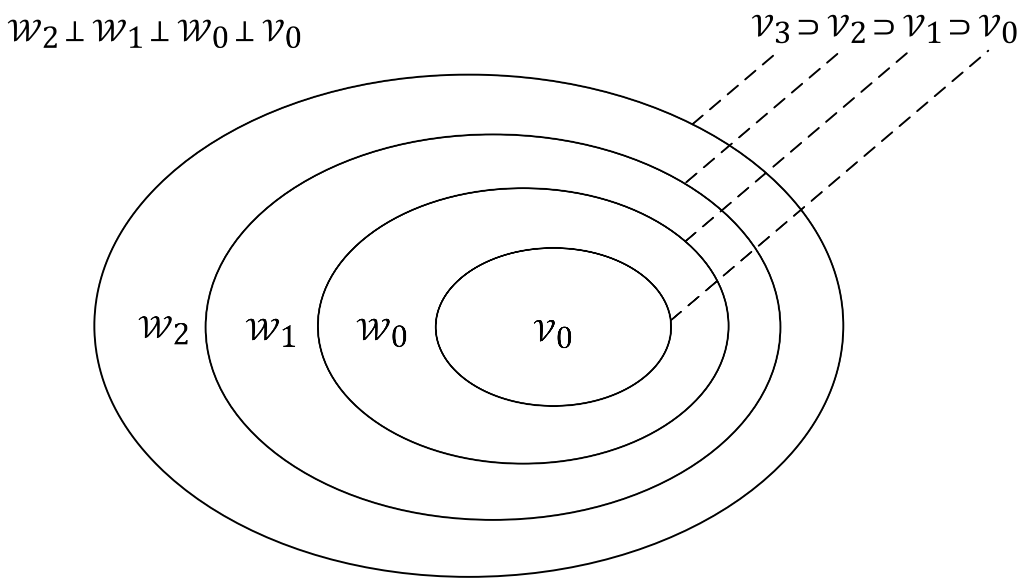

Figure 2.21: Scaling Function and Wavelet Vector Spaces

The scale of the initial space $\mathcal{V}_j$ can be chosen arbitrarily, but is usually chosen to be the coarsest detail of interest in a signal. It can even be chosen as $j = -\infty$ where L^2 can be reconstructed only in terms of wavelet functions (2.29)

$$L^2 = \cdots \oplus \mathcal{W}_{-2} \oplus \mathcal{W}_{-1} \oplus \mathcal{W}_0 \oplus \mathcal{W}_1 \oplus \mathcal{W}_2 \oplus \cdots \tag{2.29}$$

A very basic wavelet system with a scaling function and a wavelet function to make up the detail between one level of decomposition and the next is the Haar system shown in Figure 2.22.

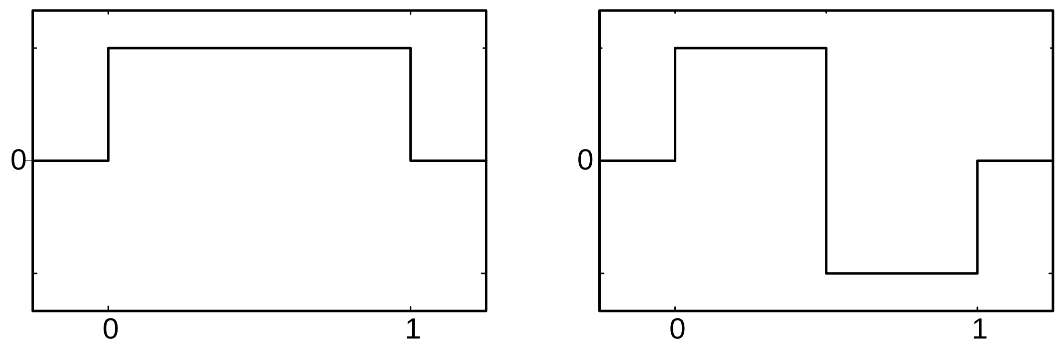

Figure 2.22: Haar scaling and Wavelet Functions

Any function in $L^2(\mathbf{R})$ can be written as an expansion of a scaling function and wavelets (2.30), where $c_{j0}(k)$ are the scaling function coefficients, $\varphi_{j0,k}(t)$ is the scaling function at the initial scale j_0, $d_j(k)$ are the wavelet function coefficients and $\psi_{j,k}(t)$ are the wavelet functions spanning the space between $\mathcal{V}_{j0}$ and L^2.

$$f(t) = \sum_{k=-\infty}^{\infty} c(k)\,\varphi_{j0,k}(t) + \sum_{k=-\infty}^{\infty}\sum_{j=j_0}^{\infty} d_j(k)\,\psi_{j,k}(t) \qquad (2.30)$$

2.5 Classification Methods

Once the feature extraction is complete, the coefficients resulting from STFT or WT need to be processed to determine the location and severity of the fault. This involves categorizing or classifying the features based on a training algorithm. Classification methods are used to classify the features from a healthy winding as ‘healthy’, and those from a faulted winding as ‘faulty’.

2.5.1 Nearest Neighbor Rule

The Nearest Neighbor Rule (NNR) is one of the simplest algorithms used for classification. In simple terms, this algorithm or rule classifies **x** by measuring its distance to nearest samples and then assign **x** the label of the corresponding nearest samples. Using this idea, a better approach would be to measure the distance of test point **x** to the mean of all samples of each class; centroid of the class. The centroid represents the weighted average of all samples. In the case of two classes, there will be two centroids. The goal is to calculate the distance of **x** to each centroid and classifying based on the smallest distance. First the classifier has to be *trained*, which is done by taking 1 sample out (test sample), from each class, calculate the centroid of remaining samples, calculate the distance of the test sample from each centroid and then classify the test sample. The choice of distance measure is important and the most common one is Euclidean distance.

Consider two classes and let $a_1, a_2, a_3, \cdots, a_k$ represent samples of class 1 and $b_1, b_2, b_3, \cdots, b_k$ represent samples of class 2.

$$Euclidean\ Distance(\boldsymbol{a}, \boldsymbol{b}) = \sqrt{(a_1 - b_1)^2 + (a_2 - b_2)^2 + \cdots + (a_k - b_k)^2} \qquad (2.31)$$

Other distance measures include the Manhattan or city-block distance, where the absolute values of samples are added up and Minkowski distance, where instead of square of distance, higher dimensions are used. In most cases, the Euclidean distance provides a good compromise and thus has been used as the distance measure for the classification method discussed here.

In our analysis, the classifier is trained with 99 out of the 100 samples, with 1 sample left out, called the test sample. A different test sample is chosen until all samples have been considered. If the test sample is from a test with faulty winding, then the centroid of fault samples is computed from the remaining 49 samples while the centroid of healthy samples is computed from all 50 samples. Vice versa, if the test sample is from a test with healthy winding. Once the classifier has been trained, the distance of every test sample (taken one at a time) to both faulty and healthy centroid is calculated. The test sample is classified into one of two classes; ‘faulty’, if the test sample lies close to fault centroid and ‘healthy’, if the test sample lies close to healthy centroid.

2.5.2 Linear Discriminant Classifier

Linear Discriminant Classifier (LDC) is trained based on the input feature vectors of a set of known faults or classes. If the feature space is divided into C sub regions, where C is the number of fault classes, then each region corresponds to a different fault severity. In order to separate the classes apart, the classifier iteratively computes weighting coefficients that maximize the linear discriminant function for that class. The linear discriminant function is defined as [9]:

$$D_C(x) = x_1\alpha_{1c} + x_2\alpha_{2c} + \cdots + x_k\alpha_{kc} + \alpha_{k+,1c} \tag{2.32}$$

$$c = 1,2,\dots,C$$

where x is the k-dimensional feature vector and α are the weighting coefficients for the C-th class. A test vector belongs to a particular class, if the discriminant function for that class is greater than the discriminant function for any other class i.e. x belongs to class j if:

$$D_j(\boldsymbol{x}) > D_k(\boldsymbol{x}),$$

for every k≠j.

Young and Calvert [10] show that the training algorithm converges in a finite number of steps. If a sample is correctly classified, then no adjustment to the weighting coefficients is made, but if samples is incorrectly classified,

$$D_j(\boldsymbol{x}) \leq D_l(\boldsymbol{x}),$$

where

$$D_l(x) = \max_{l \neq j}\left[D_1(x), \dots, D_k(x)\right],$$

adjustments are made to α_j and α_l only,

$$\alpha_j(i+1) = \alpha_j(i) + a x_i \tag{2.33}$$

$$\alpha_l(i+1) = \alpha_l(i) - a x_i \tag{2.34}$$

where a is a gain constant.

Chapter 3

Problem Formulation and Proposed Solution

3.1 Problem

The problem at hand is the detection of welding faults in the end turn windings of AC machines. These types of faults are attributed to a poor welding joint, a crack in the welding or simply deterioration of the welding over time. Early fault detection requires a good analysis tool so as to extend the life of the machine. In this work, the fault analysis of stator windings is concerned.

3.2 Motivation and Proposed Solution

The motivation of our approach is the similarity of a coil to a transmission line, and the use of the concept of reflectometry. An impulse sent at the beginning of a transmission line will cause reflections. These reflections depend on the type of termination of the line and the discontinuities in it. We will use this concept of reflectometry in the stator windings and by observing the reflections we hope to be able to detect the fault.

The study of reflectometry is based on the transmission line model under the assumption that the machine is modeled as a transmission line. The windings are modeled as transmission lines with the end windings being lumped into series resistances as shown in the figure below:

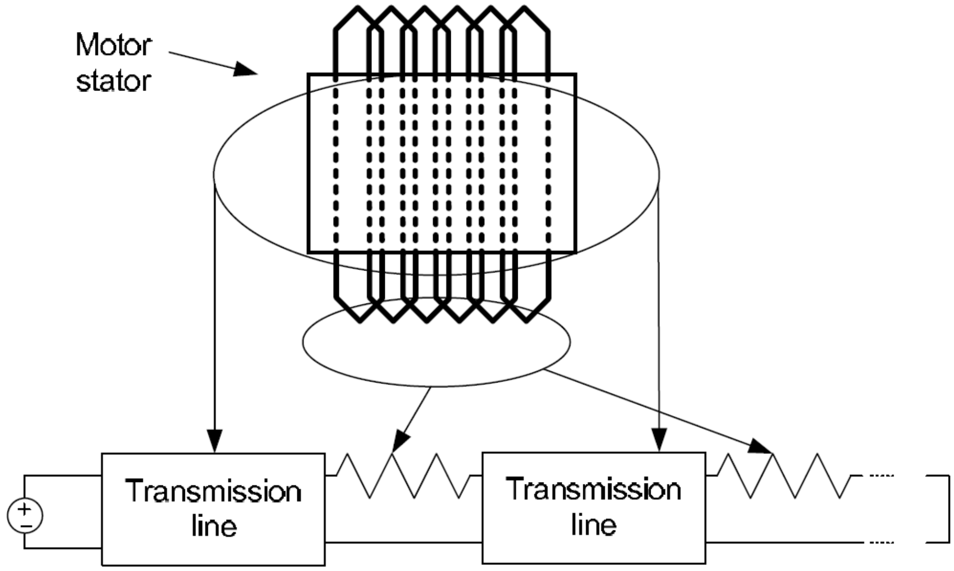

Figure 3.1: Machine Model for Impulse Test

Some assumptions that are made in the simplified model are the following:

1. The coupling capacitance between the windings is neglected
2. The mutual inductance between the phases is neglected
3. The copper bars are approximated as parallel plate transmission lines

Analyzing the windings under these assumptions makes the pulsed reflectometry easy to understand. Ideally an impulse input to the transmission line will only reflect from discontinuity in the winding. However, since the transmission line (windings) is lossy, the amplitude of the impulse is distorted and the waveform is dispersed. The reason for distortion is due to energy losses in the transmission line as the pulse propagates through it. Dispersion occurs because every end turn in the winding contributes as a small fault and causes the pulse to reflect at multiple locations. Fourier analysis of the pulse shows that there are certain frequency components that are affected more than the others. The components travel at different speeds through the winding and the initial pulse gets distorted and spreads out.

More specifically, the incident pulse reflects when it encounters a change of impedance. In a healthy transmission line, the only reflection is from the termination of the line where the load impedance is different from the characteristic impedance of the line. When a fault occurs, it acts like an additional impedance in the line. The input pulse will go through two reflections, one from the load and one from the additional discontinuity. Multiple reflections indicate the presence of a fault in a transmission line. The location of the fault can be predicted by calculating the time between incident and reflected pulses. The severity of the fault can be predicted by the attenuation in the amplitude of the input pulse.

Diagnosis techniques include the analysis of feature extraction methods and classifiers. Algorithms are developed for each one of these and a top level down system is shown below

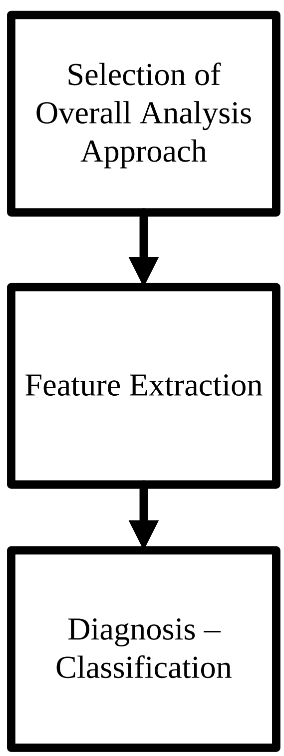

Figure 3.2: Top level down system

3.2.1 Feature Extraction Methods

Feature Extraction methods can be implemented in time domain, frequency domain or the time-frequency domain. In time domain, the features will be the voltage amplitude of the reflected pulse. This may be suitable for steady-state but to monitor small changes in transients, time domain analysis is insufficient. In frequency domain analysis, frequency spectrum is used to diagnose a fault by comparing a healthy case with a faulted case. However in case of transients, the frequency spectrum cannot indicate a fault. Time–frequency domain analysis is used inherently to detect faults in transients. Features are represented in three dimensions: time, frequency and the amplitude. There are various feature extraction methods that have been used to detect transient faults such as Short Time Fourier Transform, Wavelet Transform, Wigner Vile Distribution, Choi Williams Distribution. In this work, only the STFT and WT will be considered.

3.2.2 Classification Methods

Once the feature extraction is done, the features are input to a classifier for fault classification. There are numerous classifiers, some that are based on prior knowledge of the data and some that assume no prior information. Here we will consider the latter case that includes methods like Nearest Neighbor Rule (NNR) and Linear Discriminant Analysis (LDA). Both of these methods have been used and a comparison will be listed detailing the performance of each classifier.

Chapter 4

Experimental Setup

4.1 Experimental Setup

The experimental setup consists of the following

- HP Agilent DSO-9064A Digital Oscilloscope
- HP Pulse Generator 8012A
- Desktop PC
- SMA Cables (6” cables)
- SMA to BNC connector
- SMA ‘T’ connector
- Stator winding under test

A block diagram of the setup is shown in Figure 4.1. The 3 phase stator shown has the fault only in Phase A. Three different fault locations are considered: fault at near the pulsing end, fault at center of the winding, fault in between the near and center or fault at quarter way through the winding. Figure 4.1 shows a generic fault location. Channel-1 of the oscilloscope is connected together with the output of the Pulse Generator using a SMA ‘T’ connection ring which is then connected to Phase A. This is the setup used to test Phase A. Similarly, to test Phase B, the BNC cable is removed from Phase A terminal and connected to Phase B terminal.

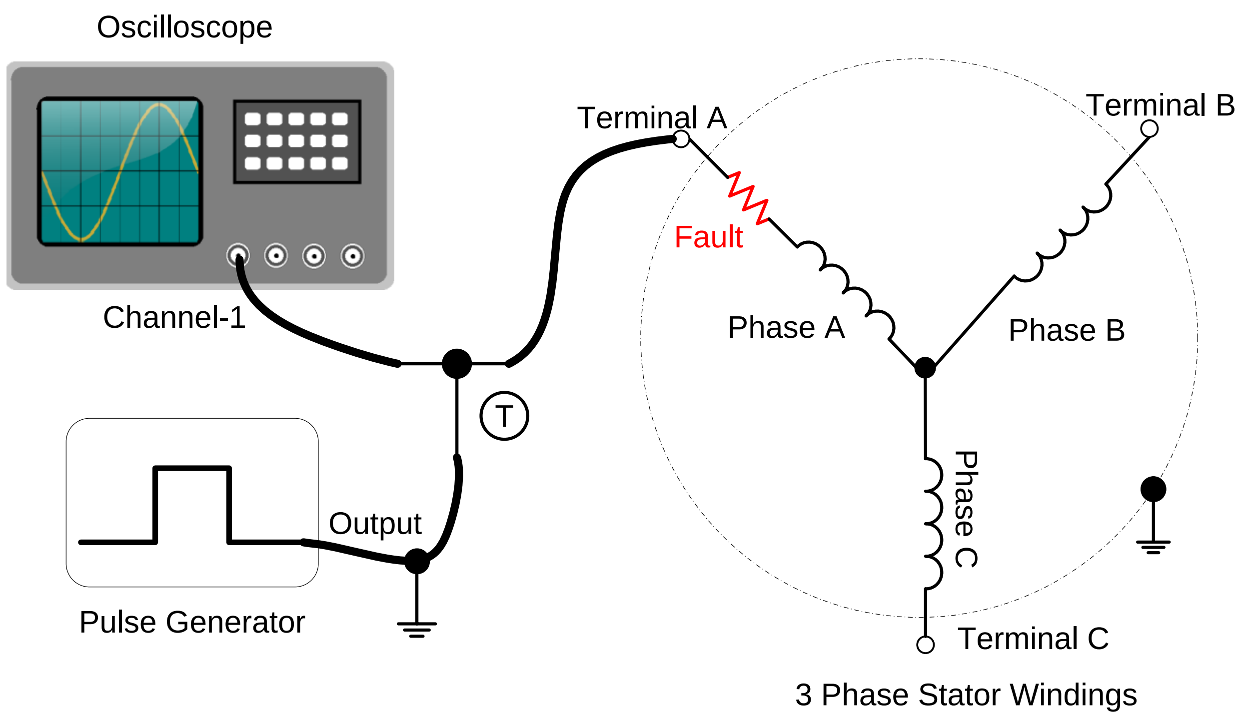

Figure 4.1: Block Diagram of system

The Pulse Generator is set to the following parameter values in Table 4.1. The width is set to the absolute minimum and the Rise Time is calculated using the Oscilloscope. Note that the scope introduces an error in the measurement that depends on its bandwidth, 600 MHz. To account for this error, the Rise Time of the scope needs to be calculated using:

$$T_{r,\,scope} = \frac{0.35}{BW} = \frac{0.35}{600MHz} = 0.583\ ns$$

The measured Rise Time of the pulse is $T_{r,\,meas} = 4.22\ ns$. The actual Rise Time is given by:

$$T_{r,\,actual} = \sqrt{\left(T_{r,\,meas}\right)^2 - \left(T_{r,\,scope}\right)^2} = \sqrt{(4.22)^2 - (0.583)^2} = 4.1795\ ns$$

Pulse Characteristics	
Magnitude	8.0 $Volts$
Width	8.0 ns
Rise Time	4.1795 ns

Table 4.1: Pulse Characteristics from Pulse Generator

4.2 Stator winding parameters

The stator winding under test is a distributed 3-phase winding with the following parameters, followed by a cross-sectional view in Figure 4.2. Only Phase A is shown with the fault at near end (location 1).

Parameter	
Winding type	distributed
Number of phases	3
Winding connection	wye
Number of slots	60
Number of conductors per slot	4
Stator outer diameter	207 mm
Stator inner diameter	155 mm

Table 4.2: Stator winding parameters

4.3 Calculations

Length Approximation:

$$sections\ of\ motor = 10$$

$$No.of\ turns/section = 12$$

$$Total\ no.of\ turns = 120$$

$$lenght\ of\ 1\ turn = 31.2\ cm$$

$$length\ of\ 120\ turns = l = 3744\ cm = 37.44\ m$$

Area Approximation:

$$cross - sectional\ area = A = 1.332 \times 10^{-5}\ m^2$$

Resistance Approximation:

$$R = \rho \frac{l}{A}$$

Where ρ = $1.68 \times 10^{-8} (\Omega \cdot m)$

Using the above results, the resistance of the winding is approximated to be:

$$R = 47.22\ m\Omega$$

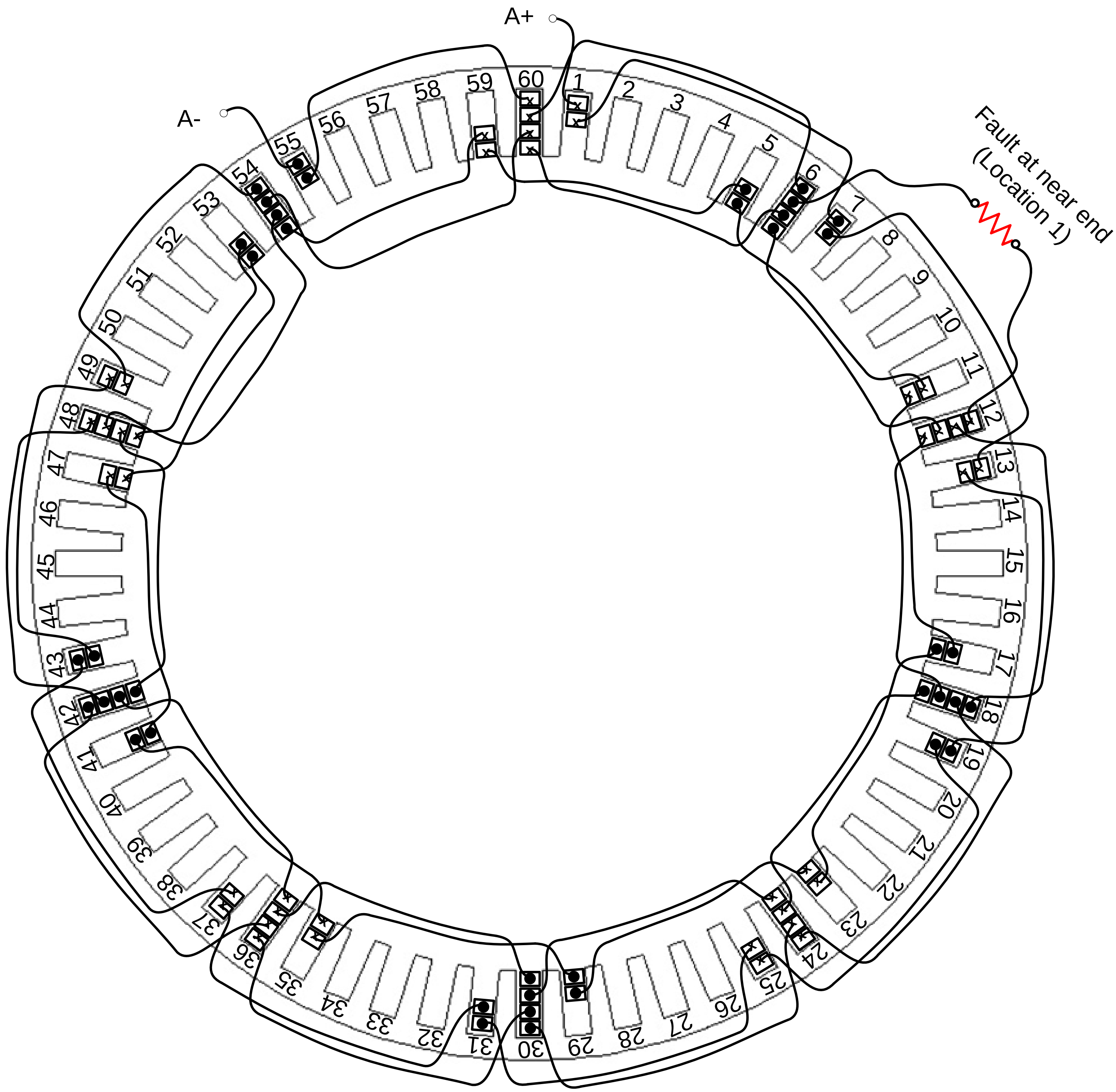

Figure 4.2: Cross sectional view of stator winding under test (Phase A shown)

4.4 Testing Procedure

The testing procedure consists of the following steps:

- Connect one end of the winding to the pulse generator
- Use a SMA 'T' connector to connect the winding to channel 1 of the scope
- Connect the other end of the winding to channel 2 of the scope
- Set the pulse generator to 'single pulse' mode and trigger the scope at the rising edge of the input pulse
- Record the data from the scope by doing repeated single pulse inputs and recording the reflected wave every time

The pulse generator is connected to the input terminals of the stator windings, which contains a fault. Using a 'T' connection ring, a scope is also connected to the input of the windings to observe the reflections. Once the input pulse travels through the winding, it will be reflected back, hopefully from the fault but there are other discontinuities in the winding (end turns) that will give unwanted reflections. The assumption here is that most of the pulse will be reflected back from the fault in the winding. Each of the end turns contributes to a fault but the actual fault will have the largest contribution. Once the scope has recorded the data, it is saved to a PC which is then used to post-process this raw data, using feature extraction techniques and classification methods.

Figure 4.3 below shows the setup of the windings. The figure on the left shows a healthy case, in which a clamp is used to hold together the open windings. The figure on the right shows a faulty case in which a terminal block is connected in series with the winding by welding it. The resistor is used to simulate a fault in this case. Multiple resistor values have been considered: 1 Ω, 0.33 Ω, 0.1 Ω and 0.027 Ω.

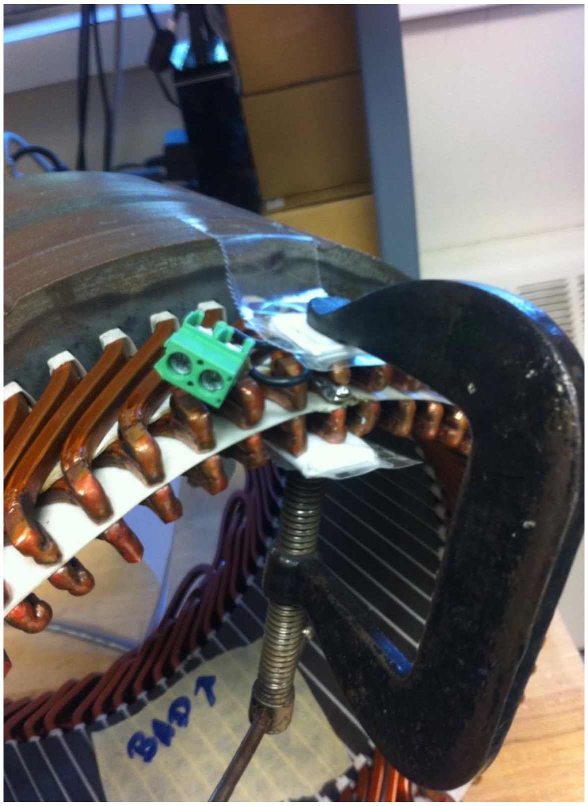

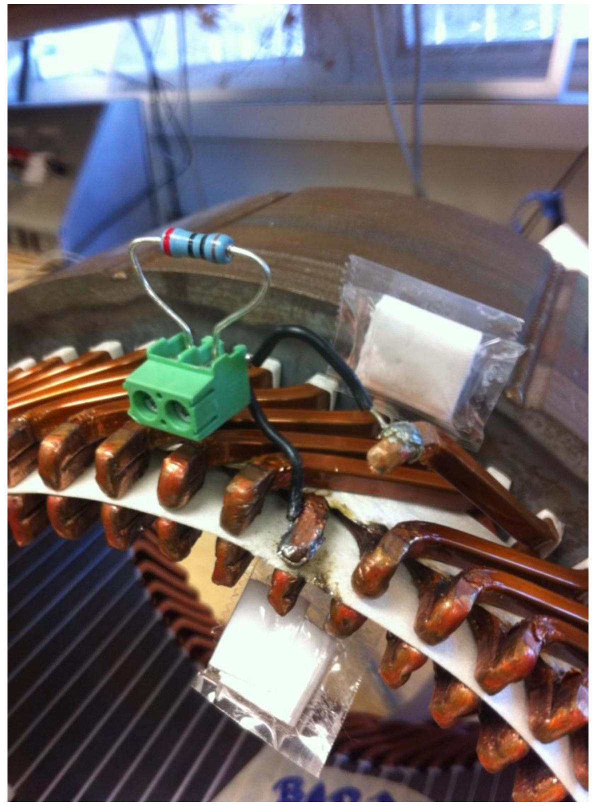

Figure 4.3: Testing healthy winding (left), faulty winding (right)

Tests are conducted with windings both healthy and containing a fault. The faults are created in three separate regions of the winding. First is the fault located closest to the pulsing end that is referred to as “Near End Fault”. Second is the fault located at the center of the winding or the “Fault at Center”. Third is the fault between the two prior faults or “Fault at Quarter”. Note that these locations are relative to the pulsing end of the winding. Another fault location can be created if the pulsing end of the windings are interchanged. More specifically, the near end fault will now appear as a “Far End Fault” with respect to the pulsing end. The objective is to use the reflections resulting from an impulse applied to a terminal, to determine the state of health and in case of a fault, the fault severity/location. For each fault location, different fault severities are considered and the same test (sending a pulse and recording the reflection) is repeated fifty times to get a total of fifty samples per fault severity per location. It is expected that by changing the fault location, the reflected pulse pattern will also change. Further the fault from the pulsing end, the longer the delay in the reflected pulse to arrive back. Figure 4.4 below shows the stator with all three faults.

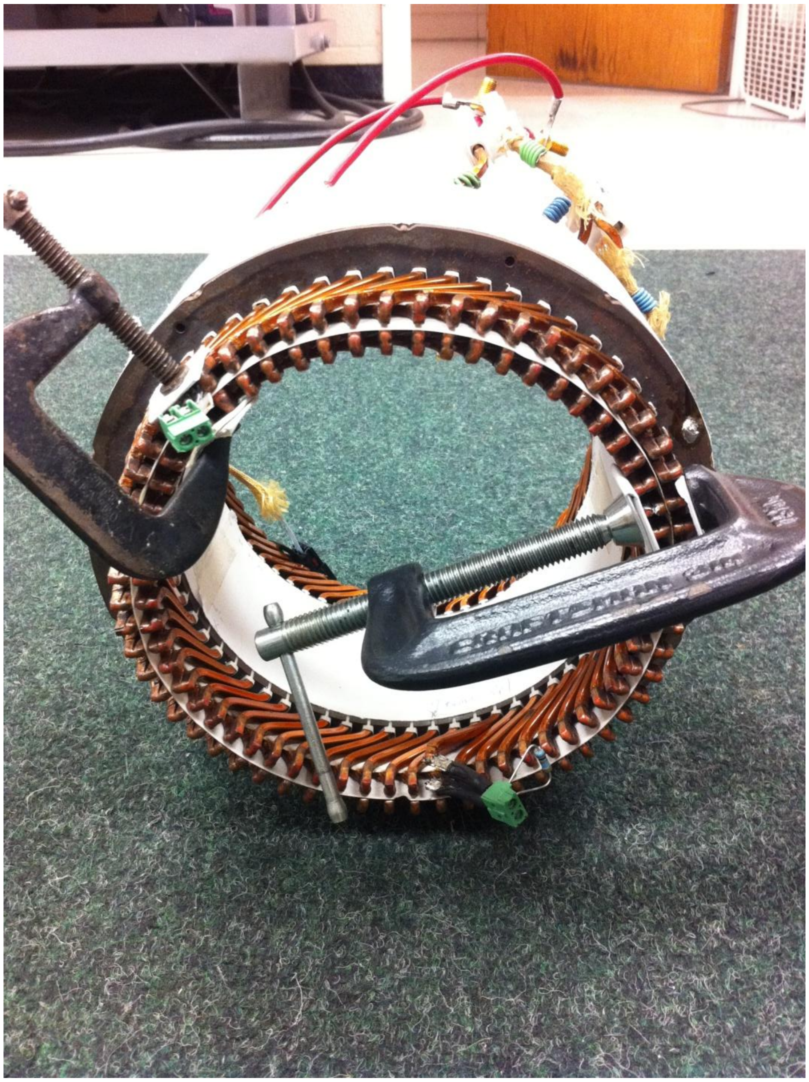

Figure 4.4: Three fault locations in the stator winding. (clamps show the actual location)

Following Table 4.3 summarizes the different test cases. Only Phase A is considered in these tests. Several fault severities are considered as mentioned before, 1.0 Ω, 0.33 Ω, 0.1 Ω and 0.027 Ω. Two test configurations are selected: Configuration 1 (C1) and configuration 2 (C2). C1 refers to the configuration in which the pulsing end of the winding is at one terminal while C2 refers to the pulsing end interchanged. State represents the state of the winding during the testing, in this case four possible states.

Case 1 is when there is no fault in the stator, or a healthy winding. To make a phase healthy, the fault locations in the winding were clamped to simulate a short. For each fault location, different fault severities were tested. Only one fault location and one fault severity is considered at a time, with the assumption being that the fault is present at only one location in the winding, during a test. This means that when testing for Fault at location 1, the other locations are clamped to avoid any unwanted reflections from other fault locations.

Cases 2 – 5 represent the fault at location 1, or Near End Fault. Cases 6 – 9 represent the fault at location 2, or Fault at center. Cases 10 – 13 represent the fault at location 3, or Fault at Quarter.

Tests	Phase	Fault Severity (Ω)	Configuration	State
Case 1	Phase A	-	C1	Healthy
Case 2	Phase A	1.0	C1	Fault at Loc 1
Case 3	Phase A	0.33	C1	Fault at Loc 1
Case 4	Phase A	0.1	C1	Fault at Loc 1
Case 5	Phase A	0.027	C1	Fault at Loc 1
Case 6	Phase A	1.0	C1	Fault at Loc 2
Case 7	Phase A	0.33	C1	Fault at Loc 2
Case 8	Phase A	0.1	C1	Fault at Loc 2
Case 9	Phase A	0.027	C1	Fault at Loc 2
Case 10	Phase A	1.0	C1	Fault at Loc 3
Case 11	Phase A	0.33	C1	Fault at Loc 3
Case 12	Phase A	0.1	C1	Fault at Loc 3
Case 13	Phase A	0.027	C1	Fault at Loc 3

Table 4.3: 13 Test Cases

Chapter 5

Results and Discussion

5.1 Overview

This section discusses the results that are obtained using the experimental setup and procedure in Chapter 4. The results are divided in several sections to provide a contrast between the different Feature Extraction Methods and Feature Classification Methods. Section 5.2 provides the time domain results that show the raw voltage waveform and the need to do time-frequency analysis. Voltage waveforms are shown for different fault severities and for couple of fault locations. Section 5.3 provides the frequency spectrum using the FFT analysis. Section 5.4 discusses the application of two different time-frequency analysis methods, Short Time Fourier Transform (STFT) and Wavelet Transform (WT). The time-frequency plots referred to as spectrogram for STFT and scalogram for WT are analyzed for healthy and various fault severities. Section 5.5 briefly discusses the feature selection method. Section 5.6 shows the application of two classification methods, Nearest Neighbor Rule (NNR) and Linear Discriminant Analysis (LDA) on the extracted features.

5.2 Time Domain waveforms

This section is concerned with the raw voltage waveform that is recorded at the pulsing end of the winding. Note that this waveform consists of multiple reflections occurring not only from the fault but from the end connections as well. In this section, several waveforms are shown for different fault severities and considering one fault location at a time. In this analysis, the assumptions are the following: known fault location and known fault severity. In practical sense, this assumption is void, but for initial analysis, it will suffice. The results and conclusions of this section determined the next course of action.

First the fault at location 1 is considered, the near end fault. Fault severities of 1 Ω, 0.33 Ω, 0.1 Ω and 0.027 Ω are considered. Using the theory of transmission lines, the input pulse will reflect back from the fault and possibly from other discontinuities (end windings). Figure 5.1 shows this case. It can be seen that the initial pulse is the same for any fault severity but after sometime the reflection pattern changes slightly for each fault severity. It is hard to tell where exactly the fault is present because the pulse sees different winding impedance with different fault severities. This results in different reflected and transmitted coefficients leading to varying amount of reflected and transmitted pulses. The same explanation is applicable to the other two fault locations, waveforms for which are shown in Figures 5.2 and 5.3.

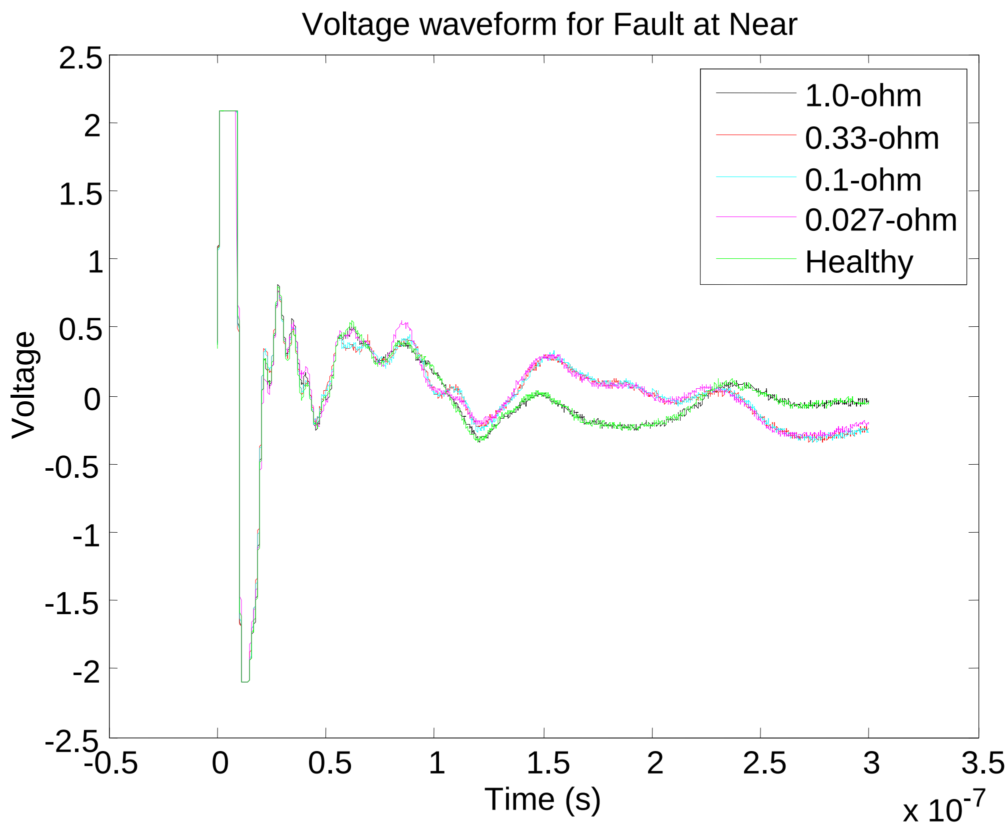

Figure 5.1: Voltage waveform for Fault at location 1

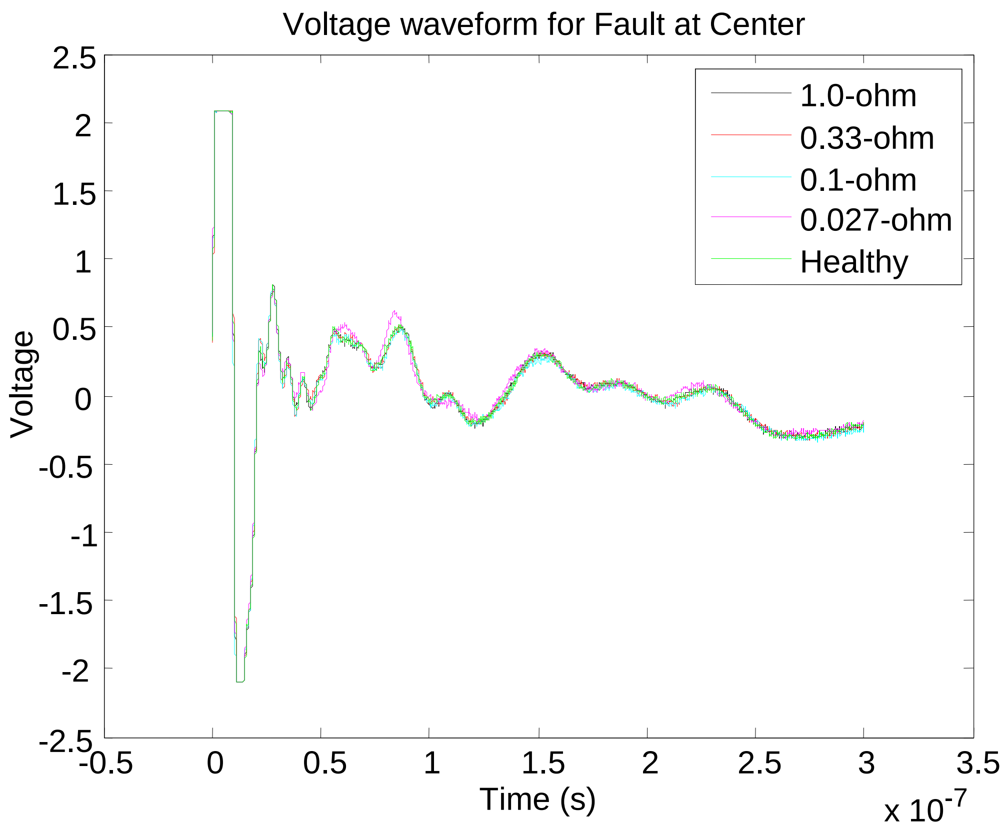

Figure 5.2: Voltage waveform for fault at location 2

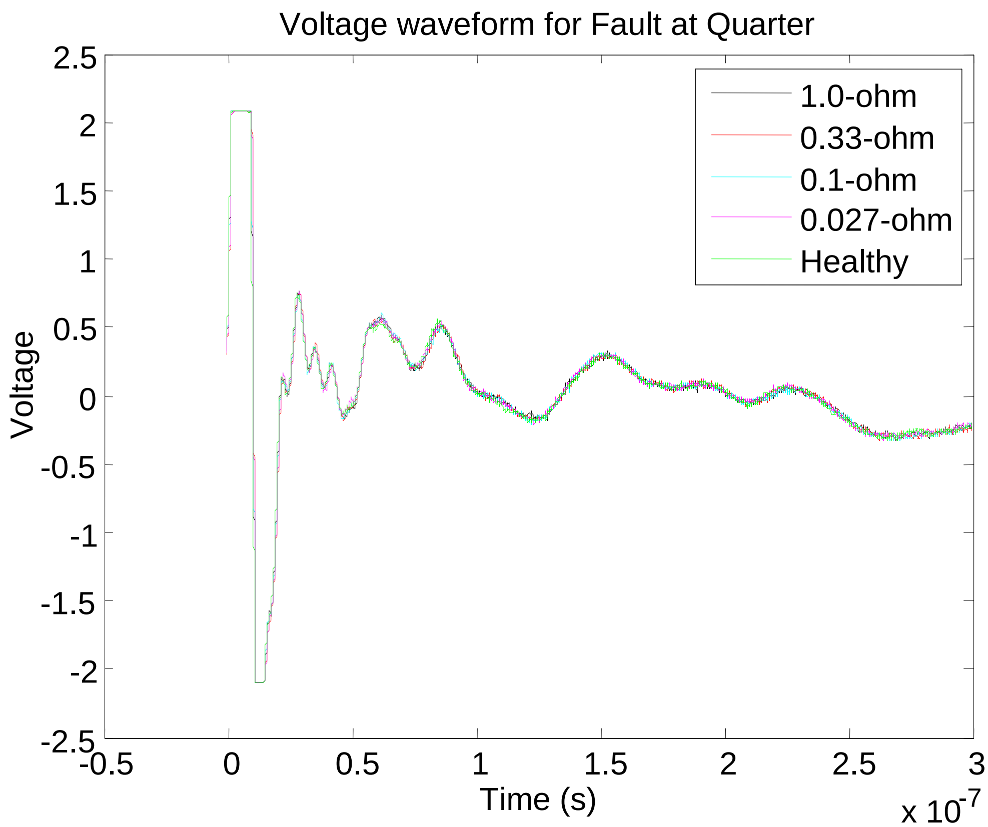

Figure 5.3: Voltage waveform for fault at location 3

It can be concluded from these preliminary results that the time domain waveforms do not provide much insight on (1) the location of the fault and (2) the severity of the fault. Based on these results, it was decided that the next approach to consider is frequency domain analysis and time-frequency analysis in which two methods are used, the STFT and the WT.

5.3 Frequency Domain waveforms

It is useful to have information about the frequency content of the time domain waveforms. Fast Fourier Transform (FFT) is used to calculate the frequency spectrum for the three different fault locations. Only fault severities of 0.1 Ω and 0.027 Ω are shown in this section. Figure 5.4 shows the frequency spectrum when fault is at location 1 or fault at near end of the winding. Figure 5.5 shows the frequency spectrum when fault is at location 2 and Figure 5.6 for fault at location 3.

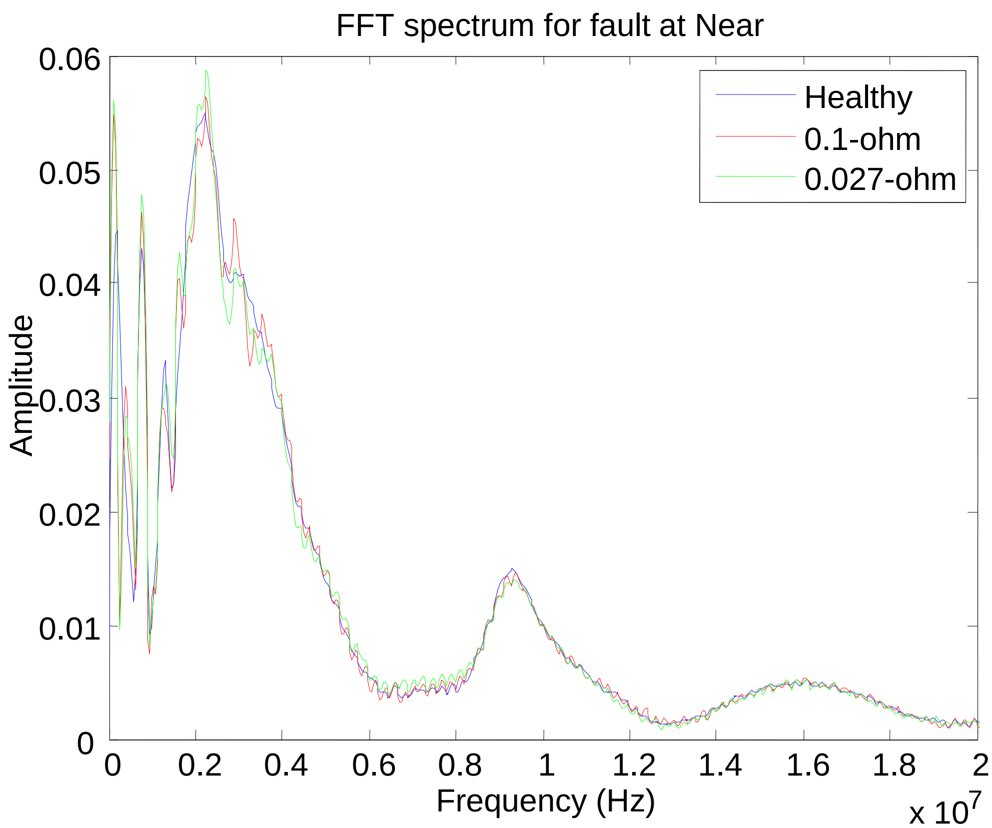

Figure 5.4: Frequency spectrum for fault at location 1

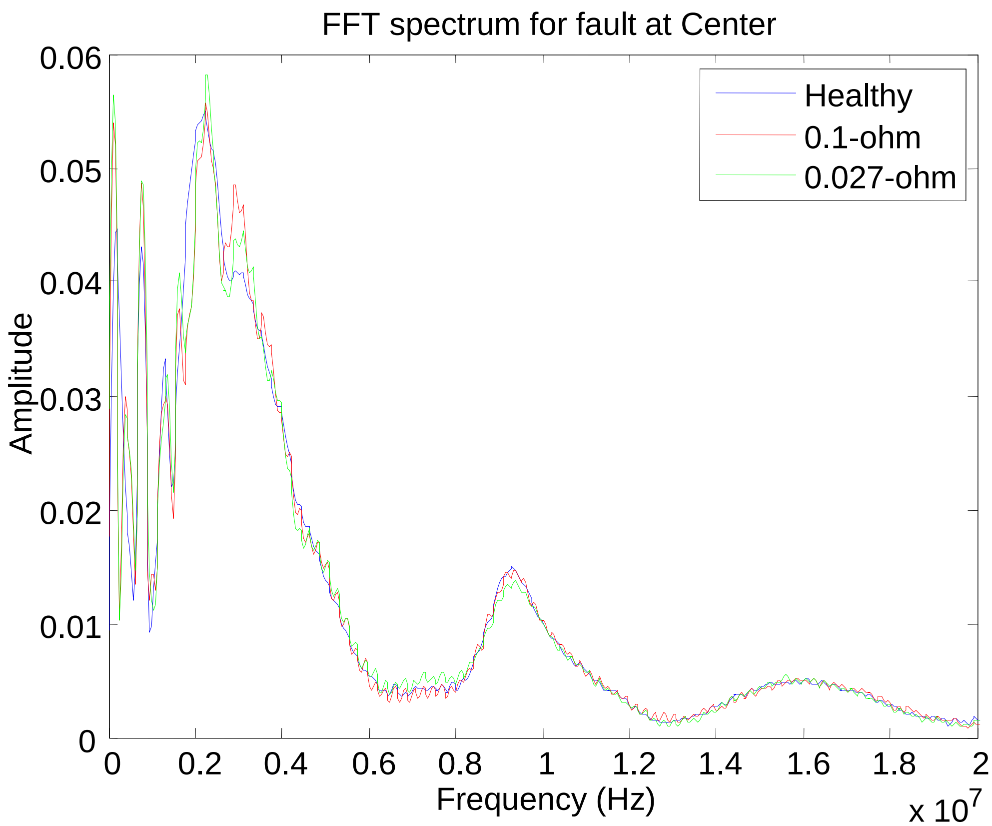

Figure 5.5: Frequency spectrum for fault at location 2

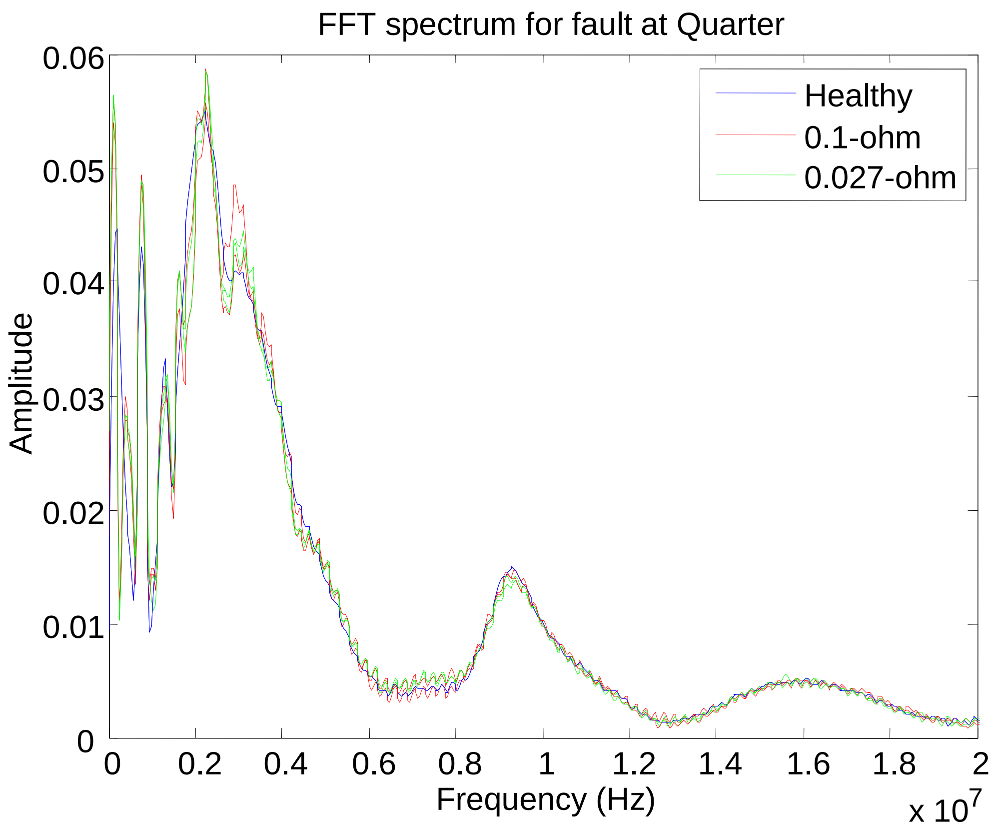

Figure 5.6: Frequency spectrum for fault at location 3

These frequency spectrums show that the dominant frequencies are present at 114.4 KHz, 419.6 KHz, 762.9 KHz and 2.289 MHz. Any higher frequencies do not contain useful information about the fault. This will be shown to hold true with time-frequency analysis as well.

5.4 Time-frequency Analysis/ Feature Extraction

The time domain waveforms alone are not enough to give a clear indication of a fault. Frequency domain waveforms only give the frequency content with no information about time. The fault information is imbedded in the measured voltage waveform but is not visible to the eye. Time-frequency analysis provides a way to view both the time and frequency content simultaneously.

5.4.1 STFT

The STFT parameter selection is important because the window length determines the location (characteristics) of the fault. Once the window length is chosen, the 'Specgram' command on MATLAB is used to compute the STFT.

[S,F,T] = Specgram(X,NFFT,FS,WINDOW,NOVERLAP)

The parameter 'S' gives a matrix that consists of the 'coefficients' of the STFT. These coefficients represent the *features* of a healthy winding when *X* is the data from a healthy winding and those of a faulty winding when *X* is the data from faulty winding. These features are important in determining the presence of a fault. Features can also be defined as the information extracted from the raw signal that are unique to it. For example, the features extracted from a healthy sample would be the same as those of another healthy sample. But the features extracted from a faulty sample, we expect to be different from the healthy case. It is of importance to note that in case of a fault, the fault is assumed to be at only one location at a time and it should ideally manifest itself in only that location. This means that the features of a healthy and faulty case should be the same for all time/frequencies except where the fault manifests itself. 'F' contains information about the frequency content of the signal while 'T' contains time information. Different fault severities are used to simulate the severity of the fault at near (location 1), fault at center (location 2), and fault at quarter (location 3) of the winding. Most severe fault is represented by 1 Ω while least severe by 0.027 Ω.

The energy of the initial pulse is the highest and decreases as the pulse travels through the winding and reflects from the fault and reaches back at the input terminal. This high energy masks any other signs of energy that can be due to the fault. To avoid this, the initial pulse is chopped out and the remaining signal is normalized with the energy that it contains. Figure 5.1 shows the voltage waveforms for different fault severities. The initial pulse is the same for all fault severities so it is acceptable to chop this part of the signal.

The need to normalize:

Normalizing is done to have a common platform for measurement, so that any inconsistency is accounted for in the experimental procedure. In this setup, the initial pulse is generated using the single-shot mode in the pulse generator. It is possible that the pulses are not identical and one pulse might be stronger than the other. Stronger in the sense of having a higher amplitude. If a pulse is stronger, then all the features after extraction will be scaled up and show a higher energy density than the features extracted from a weak pulse. This can lead to features that could potentially be different for the same fault severity for a given fault location. It is expected that the features are identical between the samples of the same fault and different between the samples of a healthy and faulty case. To normalize, all the features of a sample are divided by the total energy of the signal. The same normalizing scheme is done for all the samples. In the end, even the features that were higher (due to uneven pulses) are normalized to the same energy as the other features. This ensures that regardless of the input pulse, the features that are extracted from one fault location are all the same.

Figure 5.7 shows the spectrogram of the healthy case. The red color shows a high energy density while from yellow to blue, the energy density decreases. Most of the energy is concentrated in the lower frequency region.

Note that the spectrograms shown in this section only consider a fault severity of 0.027 Ω.

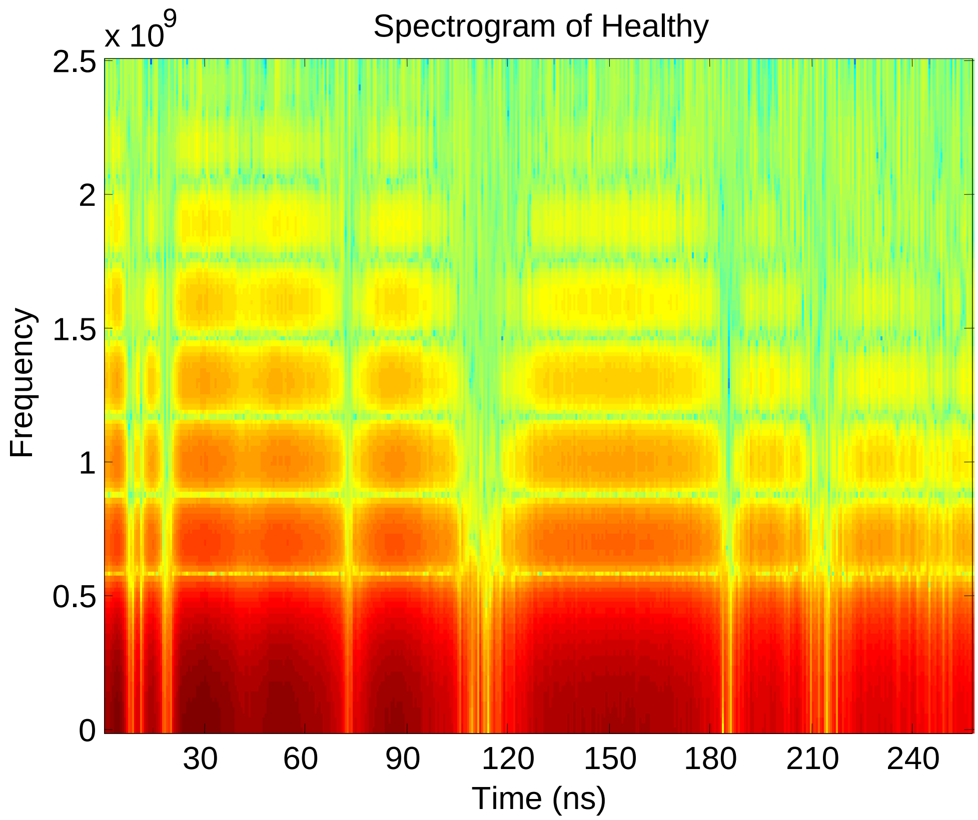

Figure 5.7: Spectrogram of Healthy case

Figure 5.8 shows the spectrogram of fault at location 1 or near end of the winding. Compared to the healthy case, the spectrograms look quite similar except at the low frequency region, i.e. below 500 MHz.

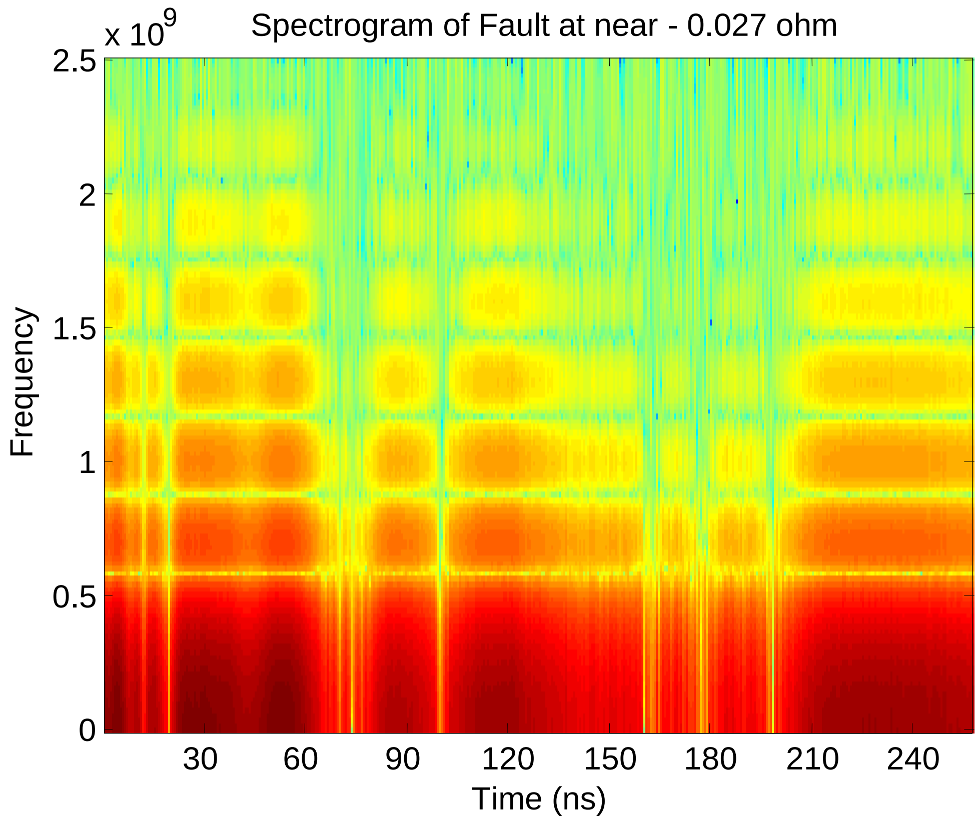

Figure 5.8: Spectrogram of Fault at near

Next, the STFT is applied to location 2 or center of the winding, to get another set of spectrogram. Same fault severity of 0.027 ohm is considered and the results are shown in Figure 5.9 below. The pattern observed at low frequencies is the same as that of before. A similar spectrogram is shown for fault at location 3 or quarter of the winding in Figure 5.10.

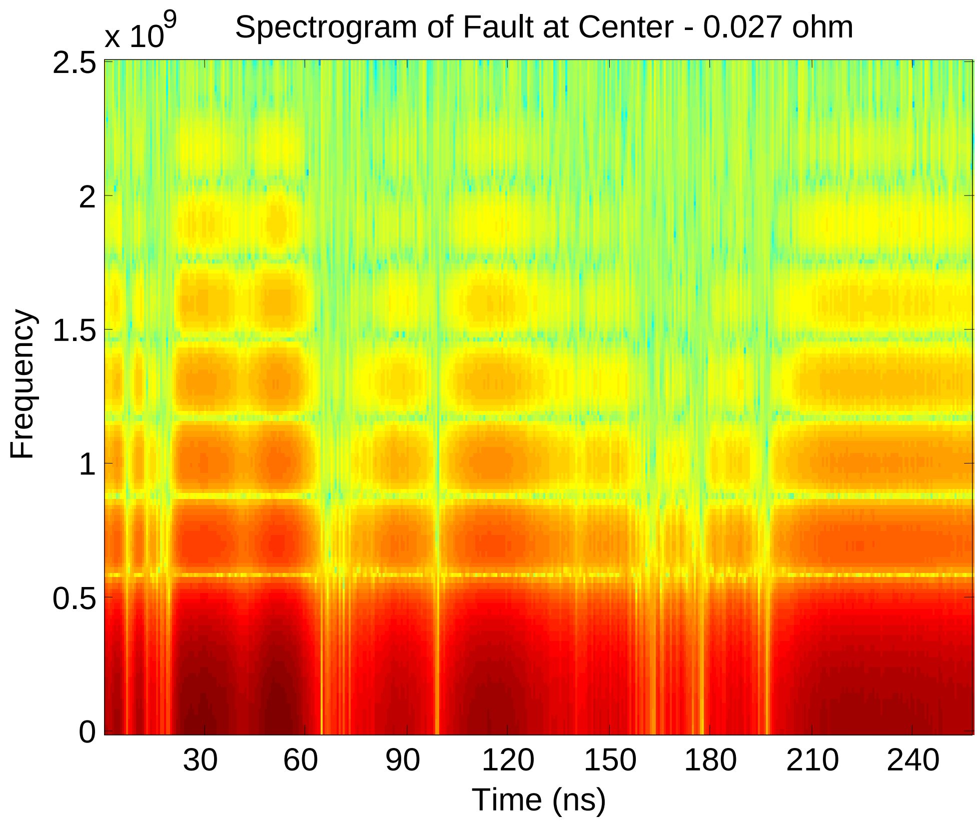

Figure 5.9: Spectrogram of Fault at center

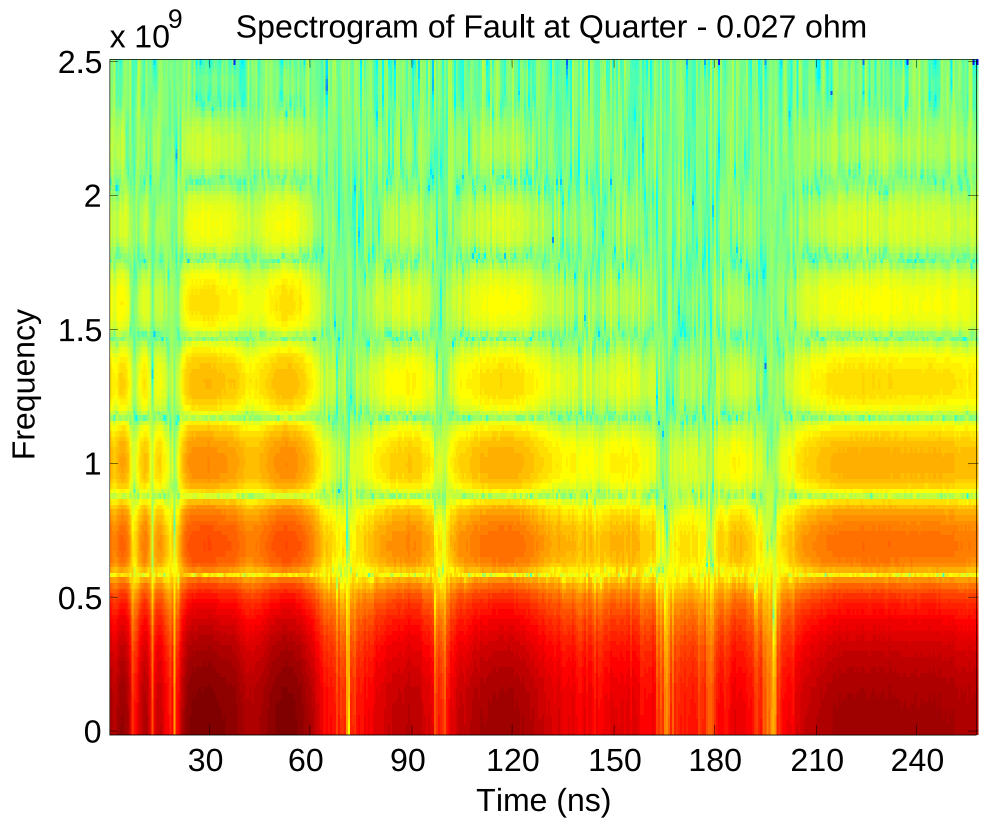

Figure 5.10: Spectrogram of Fault at quarter

The analysis based on spectrograms was only limited to observing the spectrograms. This analysis is not enough to give a clear indication of a fault in the winding. In the proceeding sections, classification methods will be discussed that use the features extracted from the STFT and classifies the winding as either healthy or faulty. But before that, Wavelet Transform is discussed next.

5.4.2 Wavelet Transform

Similar to the STFT, the WT is also a time-frequency analysis tool that offers more flexibility by providing a varying time-frequency resolution, which is a major drawback of the STFT as discussed in section 2.4.1. With wavelets, an approach similar to the STFT is adopted where the scalograms (spectrograms in STFT) are analyzed.

The selection of scales in WT is important, and it depends on the frequency content of the signal. Recall that scales are related to the inverse of frequencies. Since this work is concerned with using the Continuous Wavelet Transform (CWT), scales need to be converted to frequencies. Using the FFT, the dominant frequencies have been determined and the corresponding scales are calculated using:

$$F_a = \frac{F_c}{a.\Delta} \tag{5.1}$$

where

a = scale value

F_c = center frequency of wavelet

F_a = frequency corresponding to the scale value a, in Hz

Δ = sampling period

The wavelet used here is the Morlet wavelet shown in Figure 5.9 below. The center frequency is calculated from MATLAB using *centfrq* and comes out to be 0.8125.

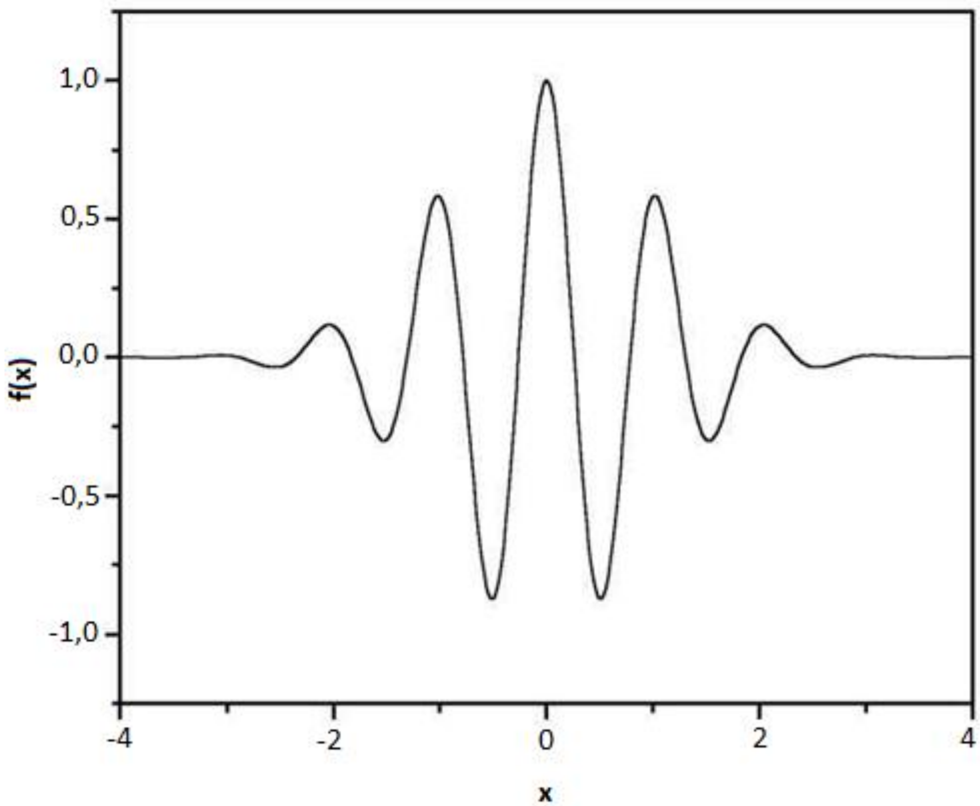

Figure 5.11: Morlet wavelet

Using (5.1) the scales that correspond to the dominant frequencies are calculated and listed in Table 5.1 below

Dominant Frequency	Corresponding Scale value
114.4 KHz	35000
419.6 KHz	9700
762.9 KHz	5300
2.289 MHz	1800

Table 5.1: Scales corresponding to dominant frequencies

The scalograms shown in this section cover a wide range of frequencies not limited to those shown in Table 5.1 to provide a complete time-frequency representation of the signal.

Note: The following figures show the scalograms for fault severity of 0.027 Ω at different fault locations. Recall that only one fault location at a time is considered during testing.

Figure 5.12 gives the scalogram of the healthy case. Same as the spectrogram, the red color represents high energy density and from yellow to blue the energy density decreases.

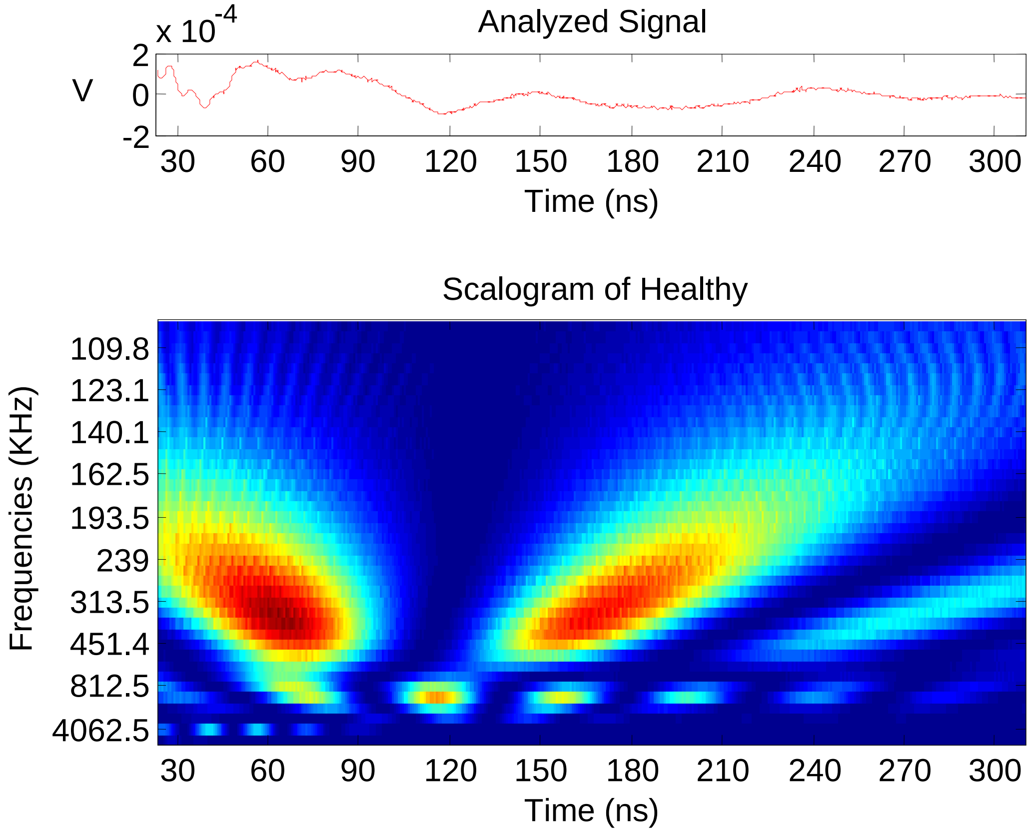

Figure 5.12: Scalogram of Healthy case

Figures 5.13 to 5.15 show the scalograms for fault at near, center and quarter respectively. It is evident that the energy density at lower frequencies is higher for all three faults, compared to the healthy case. These scalograms provide a good way to observe the time frequency content and to point out any noticeable differences between healthy and faulty cases.

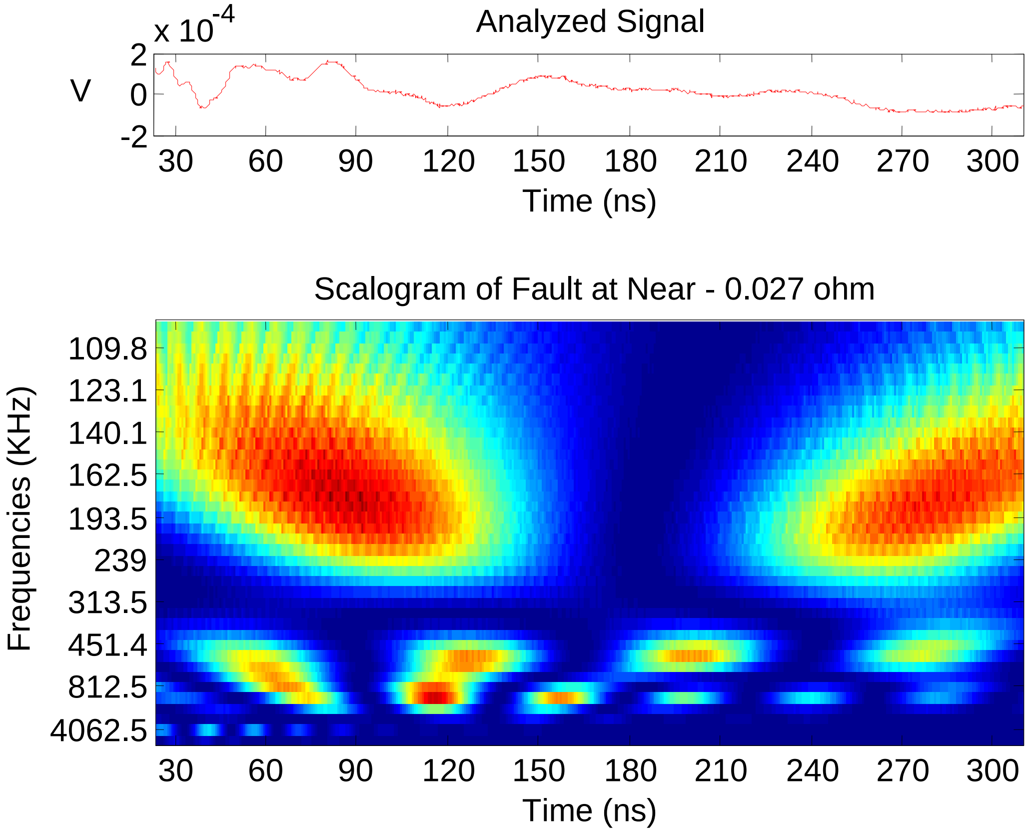

Figure 5.13: Scalogram of Fault at near

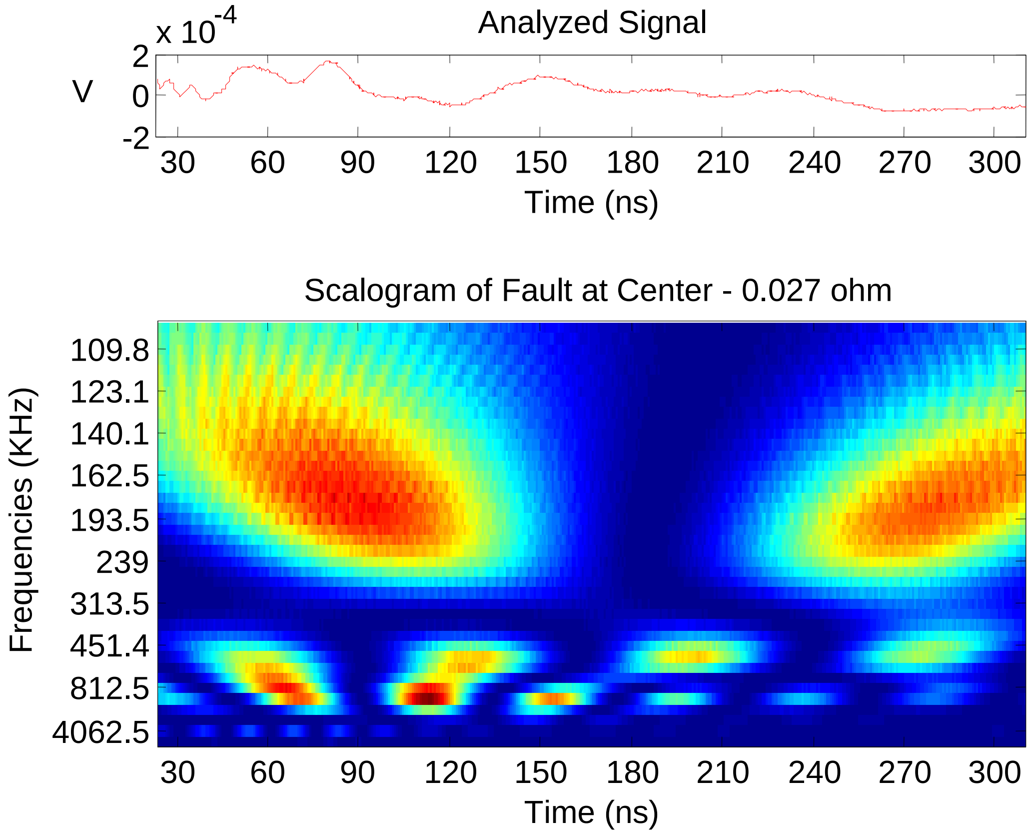

Figure 5.14: Scalogram of Fault at center

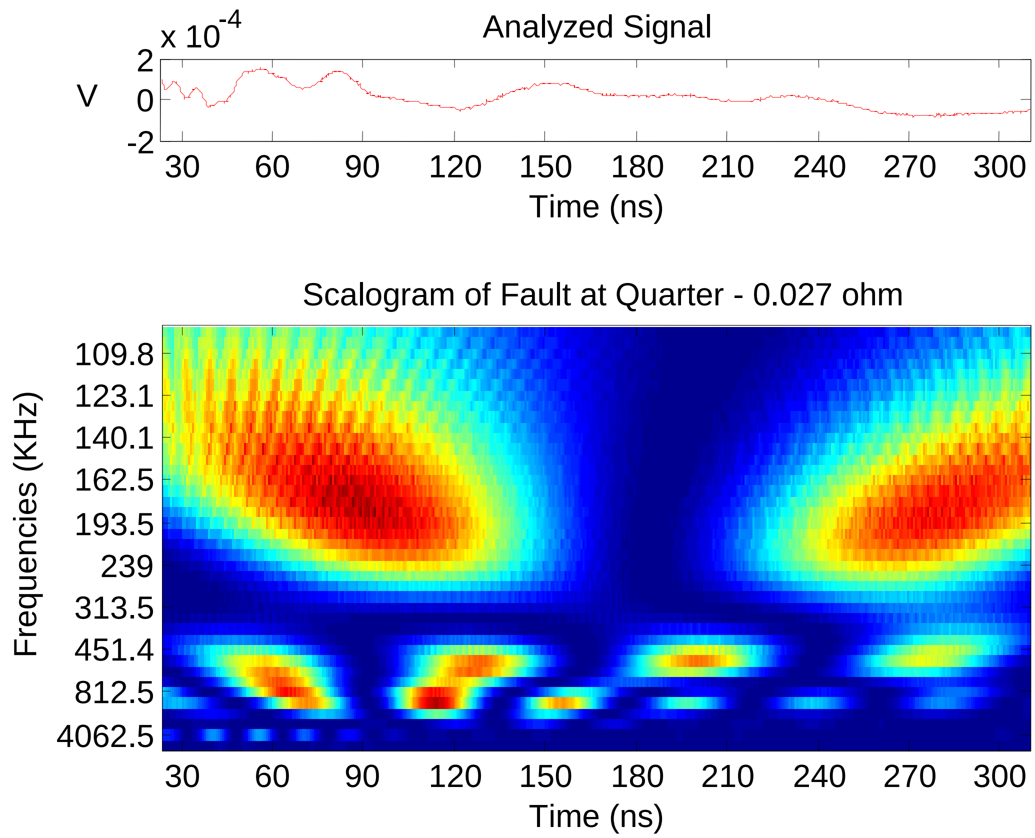

Figure 5.15: Scalogram of Fault at quarter

The feature extraction methods discussed so far provide a way to observe the features of the fault at different locations. It is shown that the pattern of the features (scalogram) changes with the presence of a fault. This is more obvious with the WT. However, based on just observation, it is hard to detect the fault. This is where classification comes in and two popular methods have been implemented, the Nearest Neighbor Rule (NNR) and the Linear Discriminant Analysis (LDA).

5.5 Feature Selection Method

Once the feature extraction is complete, the features need to be classified. However due to the dimension of the feature matrix being very large, only a few selected features that contain useful information about the fault, are chosen.

The fault is present at three different locations. These locations do not correspond to a single time instant since the fault does not manifest itself at one time. The total number of samples is 21,500 and it is not possible to select all of them. Five epochs are created each one containing 200 samples. From every epoch, 20 features are selected for a single frequency. Using the same criteria of selection for all five epochs, a total of 100 features are selected for every experiment. Each epoch corresponds to a time interval of $200 \times \frac{1}{5GHz}$ as shown in Figure 5.16 below.

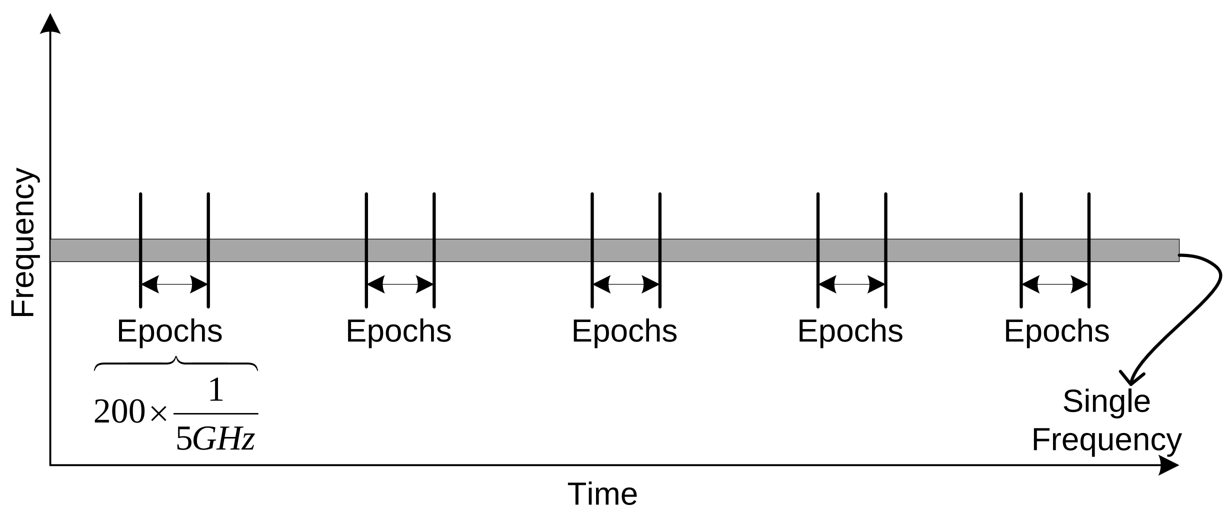

Figure 5.16: Feature selection method

The dimension of the feature matrix is large so selecting few but the right features can reduce the dimension. In case of STFT, from the spectrograms, the features corresponding to high frequencies can be neglected and only some features are considered for each fault location. The same features are chosen from the healthy case in order to compare with the faulted case. In order to see if the features of a fault and that of healthy are distinct, a classification method has to be used. Nearest Neighbor Rule and Linear Discriminant Analysis are used to classify these features in section 5.6.1. The frequencies of interest are between 2.5 MHz and 5 MHz.

In case of WT, the feature selection is based on selecting a fixed scale and all possible features corresponding to that scale. Since most of the information in the signal is carried in the lower frequencies (higher scales), only a few scales are selected, but for features that span the whole time range. The scales of interest are the same as given in Table 5.1 which are: 35000, 9700, 5300 and 1800.

5.6 Results based on Classification Methods

Classification uses the features obtained from feature extraction methods and classifies the features of a healthy winding as 'healthy' and those of a fault winding as 'fault'. In the NNR method, the mean of all healthy samples or the 'centroid of healthy' and the mean of all fault samples or the 'centroid of fault' are computed. It is expected that the centroids have the least overlap between classes. Recall that a class is defined as the samples belonging to a state of the winding. The state of the winding is healthy, fault at near end, fault at center or fault at quarter. Using Euclidean distance as a measure, samples are classified into a class based on which centroid it falls closest to. LDA however, classifies based on the discriminant function that is defined for each class during the training phase. A sample is classified into a class if the discriminant function for that class is greater than that of any other class.

5.6.1 Nearest Neighbor Rule (NNR)

5.6.1.1 NNR with feature extracted from STFT

In each of the following cases, six different time intervals are considered, in which the fault manifests itself in only one of them. The reason different time intervals are chosen, is to show by the result of the STFT and NNR classifier, that the fault manifests itself in one interval while the other five show no (or little) sign of fault.

Case 1 – 2: Near End Fault (Location 1), Fault Severity = 10 Ω (most severe), 1 Ω (least severe). The fault manifests itself in the 'Interval 1 (34 – 40 ns)'

- **Case – 1 and 2:** Fault is at location 1 with severity of 10 Ω and 1 Ω. Interval 1 (34 – 40 ns) shows that all samples of fault are close to the fault centroid and all samples of healthy are close to healthy centroid. Interval 3 shows similar results probably because this interval was chosen after interval 1 so the fault might have 'spilled over'.

NOTE: *G/F: No. of fault samples close to fault centroid
*B/F: No. of fault samples close to healthy centroid
*B/H: No. of healthy samples close to fault centroid
*G/H: No. of healthy samples close to healthy centroid

Case	Name	Fault Severity	Test Interval	Result				
				STFT	NNR			
1	Near End Fault (location 1)	10 Ω	Interval 1 (34-40 ns)		G/F*	B/F*	B/H*	G/H*
					50	0	0	50
			Interval 2 (24-30 ns)		G/F	B/F	B/H	G/H
					25	25	25	25
			Interval 3 (44-50 ns)		G/F	B/F	B/H	G/H
					49	1	0	50
			Interval 4 (78-84 ns)		G/F	B/F	B/H	G/H
					36	14	11	39
			Interval 5 (84-90 ns)		G/F	B/F	B/H	G/H
					39	11	9	41
			Interval 6 (118-124 ns)		G/F	B/F	B/H	G/H
					34	16	15	35

Case	Name	Fault Severity	Test Interval	Result				
				STFT	NNR			
2	Near End Fault (location 1)	1 Ω	Interval 1 (34-40 ns)		G/F	B/F	B/H	G/H
					48	2	0	50
			Interval 2 (24-30 ns)		G/F	B/F	B/H	G/H
					25	25	22	28
			Interval 3 (44-50 ns)		G/F	B/F	B/H	G/H
					16	34	19	31
			Interval 4 (78-84 ns)		G/F	B/F	B/H	G/H
					25	25	23	27
			Interval 5 (84-90 ns)		G/F	B/F	B/H	G/H
					28	22	29	21
			Interval 6 (118-124 ns)		G/F	B/F	B/H	G/H
					34	16	17	33

Table 5.2: STFT and NNR results for Cases 1 – 2

<u>Conclusions:</u> Based on Cases 1 – 2, the following can be concluded:

Interval	Comments
1	Fault manifests itself in this interval. Difference in spectrogram is seen and NNR classifies majority of fault samples close to fault centroid and healthy samples close to healthy centroid.
2	No fault
3	The classifier classifies majority of the fault samples (49/50) close to F centroid and all of healthy samples (50/50) close to healthy centroid. ***Possible Reason:*** *Interval 3 comes after interval 1, so it is possible that the effects of the fault were 'spilled over'.*
4	No fault
5	No fault
6	No fault

Table 5.3: Conclusions for Cases 1 – 2

Case 3 – 4: Center Fault (Location 2), Fault Severity = 10 Ω (most severe), 1 Ω (least severe).

The fault manifests itself in the 'Interval 1 (78 – 84 ns)'

- **Cases 3 and 4:** Fault is at location 2 with severity of 10 Ω and 1 Ω. For a fault severity of 10 Ω, the fault can be seen manifesting itself in interval 1; majority of fault samples (41/50) are close to the fault centroid and majority of healthy samples (42/50) are close to healthy centroid. Similarly, for a fault severity of 1 Ω, majority of fault samples (30/50) are close to the fault centroid and majority of healthy samples (34/50) are close to healthy centroid. However, the classifier performance deteriorates as the fault severity decreases.

Case	Name	Fault Severity	Test Interval	Result				
				STFT	NNR			
3	Center Fault (location 2)	10 Ω	Interval 1 (78-84 ns)		G/F	B/F	B/H	G/H
					41	9	8	42
			Interval 2 (84-90 ns)		G/F	B/F	B/H	G/H
					25	25	23	27
			Interval 3 (34-40 ns)		G/F	B/F	B/H	G/H
					27	23	20	30
			Interval 4 (24-30 ns)		G/F	B/F	B/H	G/H
					31	19	24	26
			Interval 5 (44-50 ns)		G/F	B/F	B/H	G/H
					27	23	20	30
			Interval 6 (118-124 ns)		G/F	B/F	B/H	G/H
					29	21	24	26

Case	Name	Fault Severity	Test Interval	Result				
				STFT	NNR			
4	Center Fault (location 2)	1 Ω	Interval 1 (78-84 ns)		G/F	B/F	B/H	G/H
					30	20	16	34
			Interval 2 (84-90 ns)		G/F	B/F	B/H	G/H
					23	27	24	26
			Interval 3 (34-40 ns)		G/F	B/F	B/H	G/H
					25	25	21	29
			Interval 4 (24-30 ns)		G/F	B/F	B/H	G/H
					26	24	24	26
			Interval 5 (44-50 ns)		G/F	B/F	B/H	G/H
					25	25	32	18
			Interval 6 (118-124 ns)		G/F	B/F	B/H	G/H
					29	21	24	26

Table 5.4: STFT and NNR results for Cases 3 – 4

Conclusions: Based on Cases 3 – 4, the following can be concluded:

Interval	Comments
1	Fault manifests itself in this interval. Difference in spectrogram is NOT seen but NNR classifies majority of fault samples close to fault centroid and healthy samples close to healthy centroid.
2	No fault (for 10 Ω and 1 Ω case)
3	No fault (for 10 Ω and 1 Ω case)
4	No fault (for 10 Ω and 1 Ω case)
5	No fault (for 10 Ω and 1 Ω case)
6	No fault (for 10 Ω and 1 Ω case)

Table 5.5: Conclusions for Cases 3 – 4

5.6.1.2 NNR with feature extracted from WT

Case 1 – 2: Near End Fault (Location 1), Fault Severity = 0.56 Ω and 0.33 Ω. The fault manifests itself in the 'Interval 1 (34 – 40 ns)'

- **Case – 1 and 2:** Fault is at location 1 with severity of 0.56 Ω and 0.33 Ω. No indication of fault in any interval.

Case	Name	Fault Severity	Test Interval	Result				
				WT	NNR			
1	Near End Fault (location 1)	0.56 Ω	Interval 1 (34-40 ns)		G/F	B/F	B/H	G/H
					31	19	15	35
			Interval 2 (24-30 ns)		G/F	B/F	B/H	G/H
					32	18	22	28
			Interval 3 (44-50 ns)		G/F	B/F	B/H	G/H
					31	19	28	22
			Interval 4 (78-84 ns)		G/F	B/F	B/H	G/H
					29	21	15	35
			Interval 5 (84-90 ns)		G/F	B/F	B/H	G/H
					33	17	18	32
			Interval 6 (118-124 ns)		G/F	B/F	B/H	G/H
					27	23	26	24

Case	Name	Fault Severity	Test Interval	Result				
				WT	NNR			
2	Near End Fault (location 1)	0.33 Ω	Interval 1 (34-40 ns)		G/F	B/F	B/H	G/H
					31	19	14	36
			Interval 2 (24-30 ns)		G/F	B/F	B/H	G/H
					32	18	22	28
			Interval 3 (44-50 ns)		G/F	B/F	B/H	G/H
					31	19	28	22
			Interval 4 (78-84 ns)		G/F	B/F	B/H	G/H
					31	19	17	33
			Interval 5 (84-90 ns)		G/F	B/F	B/H	G/H
					27	23	27	23
			Interval 6 (118-124 ns)		G/F	B/F	B/H	G/H
					27	23	23	27

Table 5.6: WT and NNR results for Cases 1 – 2

Case 3 – 4: Center Fault (Location 2), Fault Severity = 0.56 Ω and 0.33 Ω. The fault manifests itself in the 'Interval 1 (78 – 84 ns)'

- **Cases 3 and 4:** Fault is at location 2 with severity of 0.56 Ω and 0.33 Ω. No indication of fault in any interval.

Case	Name	Fault Severity	Test Interval	Result				
				WT	NNR			
3	Center Fault (location 2)	0.56 Ω	Interval 1 (34-40 ns)		G/F	B/F	B/H	G/H
					26	24	22	28
			Interval 2 (24-30 ns)		G/F	B/F	B/H	G/H
					26	24	22	28
			Interval 3 (44-50 ns)		G/F	B/F	B/H	G/H
					22	28	23	27
			Interval 4 (78-84 ns)		G/F	B/F	B/H	G/H
					26	24	21	29
			Interval 5 (84-90 ns)		G/F	B/F	B/H	G/H
					28	22	24	26
			Interval 6 (118-124 ns)		G/F	B/F	B/H	G/H
					5	45	45	5

Case	Name	Fault Severity	Test Interval	Result				
				WT	NNR			
4	Center Fault (location 2)	0.33 Ω	Interval 1 (34-40 ns)		G/F	B/F	B/H	G/H
					24	26	24	26
			Interval 2 (24-30 ns)		G/F	B/F	B/H	G/H
					30	20	19	31
			Interval 3 (44-50 ns)		G/F	B/F	B/H	G/H
					27	23	26	24
			Interval 4 (78-84 ns)		G/F	B/F	B/H	G/H
					28	22	24	26
			Interval 5 (84-90 ns)		G/F	B/F	B/H	G/H
					26	24	26	24
			Interval 6 (118-124 ns)		G/F	B/F	B/H	G/H
					26	24	29	21

Table 5.7: WT and NNR results for Cases 3 – 4

Final Conclusions on NNR:

Section 5.6.1.1 discusses the results of the NNR classifier with the feature extraction method being STFT. For fault located at near end, majority of the fault features are close to the fault centroid and same for the healthy case. When fault is located at center, the classifier performance deteriorates but there is still an indication of the fault, just not very pronounced. Using STFT for feature extraction of fault severity lower than 1 Ω was not very accurate, so WT was used instead for fault severities of 0.56 Ω and 0.33 Ω.

Section 5.6.1.2 discusses the results of the NNR classifier with WT as the feature extraction method. In all the cases 1 – 4, there is no indication of the fault regardless of location. It was concluded that NNR classifier, though works well for 1 Ω and higher, does not produce a promising classification for lower than 1 Ω fault severities.

This analysis was done knowing the location and severity of the fault. From a practical point of view, this method is not feasible since both the location and severity are unknown. However, this analysis helped in understanding the concept of reflectometry when applied to machines and to gain confidence in the approach.

5.6.2 Linear Discriminant Classifier (LDC)

This section discusses the results of applying the LDC to the features extracted both from the STFT and WT. In STFT, the features are extracted from a band of frequencies in the range 2.5 MHz – 5 MHz, while in WT features are extracted from four different frequencies.

The procedure for this classification method follows. The winding can be in one of multiple states but only four states are considered. First is the healthy state, defined as class 0. Then fault in the winding at near end, defined as class 1. Fault in the center of the winding, defined as class 2 and fault at quarter of the winding, defined as class 3. Total of four classes will be used in classifying the state of the winding, given a fault severity. Four fault severities of 1 Ω, 0.33 Ω, 0.1 Ω and 0.027 Ω will be used to test the performance of the classifier. Each class has 50 samples to get a total of 200 samples for all classes. The LDC computes the linear coefficients that are multiplied with the features of a class to give the discriminant of that respective class. Refer to Chapter 2, section 2.5.2 for details. If the total samples are limited then the number of features that can be used to represent a class are also limited. For example, with 200 samples, no more than 200 features per sample can be selected. This puts a serious restriction on this method due to the constraint on the number of samples.

Based on the spectrograms in section 5.4.1, it is reasonable to assume that the useful features are present in the lower frequencies so a single frequency of 2.5 MHz is chosen. Based on the scalograms in section 5.4.2, it is reasonable to assume that the useful features are concentrated in the higher scales. Scale values of 1800, 5300, 9700 and 35000 are chosen one at a time. Ideally all the features (in time) for this particular scale are used to train the classifier but due to limited samples, only a selected number of features are used. These selected features are obtained using the feature selection approach in section 5.5.

For testing the LDC, the ‘Leave 1-out method’ is used. Out of the 200 samples, 1 sample is taken out and 199 are used for training. The 1 sample is used to test the classifier to see which class it belongs to. Then a different sample is taken out of the 200 and the procedure is repeated until all 200 samples have been tested. This testing method is very convenient since the test samples are selected one by one from within the total number of samples.

The following tables summarize the results obtained from LDC for both the STFT and WT for varying fault severities. For each fault severity, four scales (frequencies) are selected in case of WT, and a single frequency in case of STFT. The samples are classified for each scale/frequency value. The total number of misclassifications are shown for each class where C 0 is healthy state, C 1 is fault at location 1, C2 is fault at location 2 and C 3 is fault at location 3. The higher the number of misclassifications, the worse is the accuracy of the classifier and the ability to detect a fault goes down.

<table>
<tr><th>Case</th><th>Feature Extraction</th><th>Frequency</th><th>Fault Severity</th><th colspan="5">No. of Misclassifications per class</th></tr>
<tr><td rowspan="8">1</td><td rowspan="8">STFT</td><td rowspan="8">F = 2.5 MHz</td><td rowspan="2">1 Ω</td><td>C 0</td><td>C 1</td><td>C 2</td><td>C 3</td><td>Total</td></tr>
<tr><td>12</td><td>11</td><td>0</td><td>0</td><td>23/200</td></tr>
<tr><td rowspan="2">0.33 Ω</td><td>C 0</td><td>C 1</td><td>C 2</td><td>C 3</td><td>Total</td></tr>
<tr><td>2</td><td>8</td><td>0</td><td>0</td><td>10/200</td></tr>
<tr><td rowspan="2">0.1 Ω</td><td>C 0</td><td>C 1</td><td>C 2</td><td>C 3</td><td>Total</td></tr>
<tr><td>14</td><td>6</td><td>0</td><td>0</td><td>20/200</td></tr>
<tr><td rowspan="2">0.027 Ω</td><td>C 0</td><td>C 1</td><td>C 2</td><td>C 3</td><td>Total</td></tr>
<tr><td>0</td><td>0</td><td>1</td><td>0</td><td>1/200</td></tr>
</table>

Table 5.8: LDC for multiple fault severities using STFT

Case	Feature Extraction	Fault Severity	Frequency/Scale	No. of Misclassifications per class				
2	WT	1 Ω	F = 114.4 KHz S = 35000	C 0	C 1	C 2	C 3	Total
				21	20	7	5	53/200
			F = 419.6 KHz S = 9700	C 0	C 1	C 2	C 3	Total
				0	0	1	1	2/200
			F = 762.9 KHz S = 5300	C 0	C 1	C 2	C 3	Total
				0	0	0	0	0/200
			F = 2.289 MHz S = 1800	C 0	C 1	C 2	C 3	Total
				0	0	0	0	0/200

Table 5.9: LDC for fault of 1 Ω using WT

Case	Name	Fault Severity	Frequency/Scale	No. of Misclassifications per class				
3	WT	0.33 Ω	F = 114.4 KHz S = 35000	C 0	C 1	C 2	C 3	Total
				17	16	2	5	40/200
			F = 419.6 KHz S = 9700	C 0	C 1	C 2	C 3	Total
				14	12	0	0	26/200
			F = 762.9 KHz S = 5300	C 0	C 1	C 2	C 3	Total
				0	0	0	0	0/200
			F = 2.289 MHz S = 1800	C 0	C 1	C 2	C 3	Total
				0	0	0	0	0/200

Table 5.10: LDC for fault of 0.33 Ω using WT

Case	Name	Fault Severity	Frequency/Scale	No. of Misclassifications per class				
4	WT	0.1 Ω	F = 114.4 KHz S = 35000	C 0	C 1	C 2	C 3	Total
				12	12	0	0	38/200
			F = 419.6 KHz S = 9700	C 0	C 1	C 2	C 3	Total
				5	6	0	0	11/200
			F = 762.9 KHz S = 5300	C 0	C 1	C 2	C 3	Total
				0	0	0	0	0/200
			F = 2.289 MHz S = 1800	C 0	C 1	C 2	C 3	Total
				0	0	0	0	0/200

Table 5.11: LDC for fault of 0.1 Ω using WT

The winding resistance was calculated to be around 47 mΩ, using $R = \rho \frac{l}{A}$. Once the LDA was tested with fault severities of down to 0.1Ω and the results were promising, the next step was to test with a fault severity of less than the winding resistance, chosen to be 0.027 Ω in this case. The results for this case are shown in table 5.11 below.

Case	Name	Fault Severity	Frequency/Scale	No. of Misclassifications per class				
5	WT	0.027 Ω	F = 114.4 KHz S = 35000	C 0	C 1	C 2	C 3	Total
				12	12	0	0	24/200
			F = 419.6 KHz S = 9700	C 0	C 1	C 2	C 3	Total
				0	1	2	1	4/200
			F = 762.9 KHz S = 5300	C 0	C 1	C 2	C 3	Total
				0	0	0	0	0/200
			F = 2.289 MHz S = 1800	C 0	C 1	C 2	C 3	Total
				0	0	0	0	0/200

Table 5.12: LDC for fault of 0.027 Ω using WT

Chapter 6

Conclusions and Future Work

The objective of this work was to provide a framework to help detect welding faults in stator windings of AC motors. The motivation of our approach was to use the concept of transmission line theory and apply it to stator windings. Pulsed reflectometry explains that any discontinuity or fault gives a specific reflection pattern that is related directly to the location and severity of the fault. The ability to classify faults, into separate classes was part of the objective as well.

Feature extraction and classification methods have been discussed along with supporting results. Certain fault severities were assumed along with specific fault locations that were created in the stator winding. The techniques developed in this work, though work for these specific cases, but can be generalized to fault at any location of any severity.

Results based on the different methods have been discussed and compared. Among the two feature extraction methods, the STFT and WT, the energy density comparison showed that features from WT are more discriminative (between a healthy and faulty case). Categorization schemes such as NNR and LDA provide a way to classify the extracted features into one of the fault classes, or a healthy class when no fault is present. LDA proved to be a better and accurate classifier since fault severities as low as 0.027 Ω were distinguishable from a healthy case. Results based on LDA show that WT is the preferred extraction method since the features are classified into respective classes with higher accuracy compared to those of the STFT. Ideally, for a given fault severity, the classifier will be able to classify samples of fault from any fault location, however due to restrictions on computation, features from four classes were chosen to represent four different fault locations.

Some possible improvements involve a systematic selection of features rather than creating epochs to select the features. A simple way is to use energy thresholds, where only features above a certain threshold will be selected. Implement other Feature Extraction methods like the Wigner Ville and Choi Williams Distributions and other Feature Classification methods that require fewer samples, less training and are more sensitive.

APPENDIX

APPENDIX

```
% Name:              FFT to find dominant frequencies
% Author:            Arslan Qaiser
% Last modified:     11/30/2012

disp('==================================================================== ')

T = 2e-10;                          % Sampling Time = 1/Fs
L = 100000;                         % Defines the resolution of FFT
% Define the signals of which FFT is required
V_f2 = f_27mohm_1(:,2);
V_f1 = f_point1ohm_1(:,2);
V_h = s_1(:,2);

FS=1/T;                             % Sampling Frequency
t=(0:L-1)*T;                        % Time scale
NFFT=2^nextpow2(L);                 % NFFT for the signal
f=FS/2*linspace(0,1,NFFT/2+1);      % Frequency range for the signal

FFT_f1 = fft(V_f1,NFFT)/L;          % 0.1 mohm
FFT_f2 = fft(V_f2,NFFT)/L;          % 0.027 ohm
FFT_h = fft(V_h,NFFT)/L;            % Healthy
FFT_Sf1=2*abs(FFT_f1(1:NFFT/2+1));
FFT_Sf2=2*abs(FFT_f2(1:NFFT/2+1));
FFT_Sh=2*abs(FFT_h(1:NFFT/2+1));

figure(1)
    plot(f,FFT_Sh)
    hold on;
    plot(f,FFT_Sf1,'r')
    plot(f,FFT_Sf2,'g')
    title('FFT spectrum for fault at Quarter','FontSize',12)
    xlabel('Frequency (Hz)','FontSize',12)
    ylabel('Amplitude','FontSize',12)
    h=legend('Healthy','0.1-ohm','0.027-ohm')
    set(h,'FontSize',12)
    xlim([0 2e7])
```

```
% Name:              CWT Feature Extraction
% Author:            Arslan Qaiser
% Last modified:     11/15/2012
% Case:              Near end
%%%%%%%%%%%%%%%%%%%%%%%%%    1    %%%%%%%%%%%%%%%%%%%%%%%%%%%
vrb = cell(50,1);                    %   This defines the length of samples
%%% For Loop to generate the fault data
for i = 1:length(vrb)
   vrb{i}=genvarname(strcat('sub_10ohm_',num2str(i)));
   eval([vrb{i} '= f_1ohm_' num2str(i) '(1:24000,2);']);
end
%%% For Loop to generate the healthy data
for i = 1:length(vrb)
   vrb{i}=genvarname(strcat('sub_s_',num2str(i)));
   eval([vrb{i} '= s_' num2str(i) '(1:24000,2);']);
end

%%%%%%%%%%%%%%%%%%%%%%%%%    2    %%%%%%%%%%%%%%%%%%%%%%%%%%%
for i = 1:50
eval(['cutf' num2str(i) '=sub_10ohm_' num2str(i) '(2501:24000);'])
eval(['cuts' num2str(i) '=sub_s_' num2str(i) '(2501:24000);'])
eval(['Es' num2str(i) '=sum(abs(cuts' num2str(i) '));'])
eval(['Ef' num2str(i) '=sum(abs(cutf' num2str(i) '));'])
eval(['normf' num2str(i) '=cutf' num2str(i) '/Es' num2str(i) ';'])
eval(['norms' num2str(i) '=cuts' num2str(i) '/Es' num2str(i) ';'])
end
%
clear cut* sub*
%%%%%%%%%%%%%%%%%%%%%%%%%    3    %%%%%%%%%%%%%%%%%%%%%%%%%%%
% Feature Extraction
for i = 1:50
    eval(['feature_1ohm_' num2str(i) '_near = cwt(normf' num2str(i) ',[1800
5300 9700 35000],''morl'');'])
    eval(['feature_s_' num2str(i) ' = cwt(norms' num2str(i) ',[1800 5300 9700
35000],''morl'');'])
    disp(['done for near sample # = ' num2str(i) ])
end
```

```
% Name:             STFT Feature Extraction
% Author:           Arslan Qaiser
% Last modified:    12/12/2012
% Case:             Near end
%%%%%%%%%%%%%%%%%%%%%%%%%%    1    %%%%%%%%%%%%%%%%%%%%%%%%%%%%
vrb = cell(50,1);
%%% For Loop to generate the fault data
for i = 1:length(vrb)
   vrb{i}=genvarname(strcat('sub_10ohm_',num2str(i)));
   eval([vrb{i} '= f_1ohm_' num2str(i) '(1:24000,2);']);
end
%%% For Loop to generate the healthy data
for i = 1:length(vrb)
   vrb{i}=genvarname(strcat('sub_s_',num2str(i)));
   eval([vrb{i} '= s_' num2str(i) '(1:24000,2);']);
end

%%%%%%%%%%%%%%%%%%%%%%%%%%    2    %%%%%%%%%%%%%%%%%%%%%%%%%%%%
for i = 1:50
eval(['cutf' num2str(i) '=sub_10ohm_' num2str(i) '(2501:24000);'])
eval(['cuts' num2str(i) '=sub_s_' num2str(i) '(2501:24000);'])
eval(['Es' num2str(i) '=sum(abs(cuts' num2str(i) '));'])
eval(['Ef' num2str(i) '=sum(abs(cutf' num2str(i) '));'])
eval(['normf' num2str(i) '=cutf' num2str(i) '/Es' num2str(i) ';'])
eval(['norms' num2str(i) '=cuts' num2str(i) '/Es' num2str(i) ';'])
end
%
clear cut* sub*
%%%%%%%%%%%%%%%%%%%%%%%%%%    3    %%%%%%%%%%%%%%%%%%%%%%%%%%%%
% Feature Extraction
for i = 1:50
    eval(['temp_' num2str(i) ' = specgram(normf' num2str(i)
',2000,5e9,16,15);'])
    eval(['feature_1ohm_' num2str(i) '_near = temp_' num2str(i) '(2,:);'])
    clear temp*
    eval(['temp_' num2str(i) ' = specgram(norms' num2str(i)
',2000,5e9,16,15);'])
    eval(['feature_s_' num2str(i) ' = temp_' num2str(i) '(2,:);'])
    clear temp*
    disp(['done for near sample # = ' num2str(i) ])
end
```

```
% Name:             Linear Discriminant Classifier
% Author:           Arslan Qaiser
% Last modified:    11/15/2012
%
% How to use:
% ============================================
% - Arrange the extracted features in a vector form
% - Depending on the fault severity, change the variable name to
%   appropriate fault severity. E.g fault = 0.027 ohm, name the
%   variable 'feature_27mohm_i_near' where i=[1:50]
% - FV_H, FV_F1, FV_F2, FV_F3 contain the features for the
%   healthy and different fault locations
% - Apply the LDC using Leave 1-out method by MATLAB function CLASSIFY
%   - CLASS = CLASSIFY(SAMPLE,TRAINING,GROUP,TYPE)
%   - Use this function repeatedly for all test samples. Each time
%     CLASS gives a single number corresponding to the discriminant
%     of the respective class that the test sample belongs to.
%
% ============================================
%
%
% Defining features for Class H,F1,F2,F3
FV_H=[]; FV_F1=[]; FV_F2=[]; FV_F3=[];
num_sam = 200;
% Creating the epochs for a total of 100 features
col = [1001:10:1200 3001:10:3200 6001:10:6200 8001:10:8200 10001:10:10200];

for i=1:num_sam/4
% %--------------------- 0.027 ohm ------------------------------------
eval(['A' num2str(i) '=feature_s_' num2str(i) '(1,[col]);'])
eval(['B' num2str(i) '=feature_27mohm_' num2str(i) '_near(1,[col]);'])
eval(['C' num2str(i) '=feature_27mohm_' num2str(i) '_center(1,[col]);'])
eval(['D' num2str(i) '=feature_27mohm_' num2str(i) '_quarter(1,[col]);'])

eval(['t = reshape(A' num2str(i) ',1,length(col));'])
eval(['u = reshape(B' num2str(i) ',1,length(col));'])
eval(['v = reshape(C' num2str(i) ',1,length(col));'])
eval(['w = reshape(D' num2str(i) ',1,length(col));'])
eval('FV_H = vertcat(FV_H,t);')
eval('FV_F1 = vertcat(FV_F1,u);')
eval('FV_F2 = vertcat(FV_F2,v);')
eval('FV_F3 = vertcat(FV_F3,w);')
end

% Complete Feature Set that represents features from Class H,F1,F2,F3
FV_all = [FV_H;FV_F1;FV_F2;FV_F3];
size(FV_all);
l = length(FV_all);
l=200;
C=[];

% Applying the LDC
for idx = 1:1:l;
    sample = FV_all(idx,:);
    test = FV_all;
    test(idx,:) = [];
```

```
    training = test;
    if idx<=l/4
        group = [zeros(l/4-1,1); ones(l/4,1); 2*ones(l/4,1); 3*ones(l/4,1)];
    elseif idx>l/4 && idx<=l/2
        group = [zeros(l/4,1); ones(l/4-1,1); 2*ones(l/4,1); 3*ones(l/4,1)];
    elseif idx>l/2 && idx<=l*3/4
        group = [zeros(l/4,1); ones(l/4,1); 2*ones(l/4-1,1); 3*ones(l/4,1)];
    else
        group = [zeros(l/4,1); ones(l/4,1); 2*ones(l/4,1); 3*ones(l/4-1,1)];
    end
    [class err post logp coef] = classify(sample,training,group,'linear');
    test_class = class;
    C = vertcat(C,test_class);
%    pause
end
Final_Class = horzcat(C(1:l/4),C(l/4+1:l*(1/2)), C(l/2+1:l*(3/4)),
C(l*(3/4)+1:l))
C_0=Final_Class(:,1); C_1=Final_Class(:,2); C_2=Final_Class(:,3);
C_3=Final_Class(:,4);

disp('-----------------------------------------------')
disp(['No. of samples misclassed in Class-0: ',num2str(l/4-sum(C_0==0)),' /
50'])
disp(['No. of samples misclassed in Class-1: ',num2str(l/4-sum(C_1==1)),' /
50'])
disp(['No. of samples misclassed in Class-2: ',num2str(l/4-sum(C_2==2)),' /
50'])
disp(['No. of samples misclassed in Class-3: ',num2str(l/4-sum(C_3==3)),' /
50'])
disp('-----------------------------------------------')
disp(['Total No. of samples misclassed: ',num2str(l-
(sum(C_0==0)+sum(C_1==1)+sum(C_2==2)+sum(C_3==3))),' / 200'])
disp('-----------------------------------------------')
```

BIBLIOGRAPHY

BIBLIOGRAPHY

[1] “IEEE Guide for Transformer Impulse Tests”, IEEE Std C57.98-1993(R1999), pp.1 – 59, 1994

[2] “IEEE recommended practice for routine impulse test for distribution transformers”, IEEE Std C57.138-1998, pp. 1 – 50, 1998

[3] M. Naderi, G. Gharehpetian, M. Abedi, and T. Blackburn, “Modeling and Detection of Transformer Internal Incipient Fault during Impulse Test”, *IEEE Transactions on Dielectrics and Electrical Insulation*, vol. 15, no. 1, pp. 284 – 291, Feb. 2008.

[4] S. Porkar, G. B. Gharehpetian and K. Feser, “A disc-to-disc breakdown and arc modeling method for fault diagnosis of power transformers during impulse testing”, Springer-Verlag, Electrical Engineering Journal, ISSN: 0948-7921, Vol. 86, pp. 261-265, 2004.

[5] E. Al-Ammar, G. Karady, and H, Sim, “Novel Technique to Improve the Fault Detection Sensitivity and Transformer Impulse Test”, *IEEE Transactions on Power Delivery*, vol. 23, no. 2, pp. 717 – 725, Apr. 2008.

[6] E. Al-Ammar, G. Karady, “Transfer Function Analysis Using STFT for Improvement of the Fault Detection Sensitivity in Transformer Impulse Test”, *IEEE Transactions on Power Delivery*, 2005.

[7] P. Purkait, “Pattern classification of impulse faults in transformers by wavelet analysis,” IEEE Transactions on Dielectrics and Electrical Insulation, vol. 9, no. 4, pp. 555 – 561, Aug. 2002.

[8] C.S. Burrus, R.A. Gopinath, and H. Guo. *Introduction to Wavelets and Wavelet Transforms: A Primer.* Prentice Hall, 1998.

[9] R. O. Duda, P.E. Hart, and D.G. Stork, “Pattern Classification”, 2nd Ed, Wiley Interscience, Oct 2000

[10] Young and Calvert, “Pattern Estimation and Classification”

[11] Zanardeli, W. 2000, “The Use of Wavelet Analysis for the Prognosis of Failures in Electrical Machines”. Unpublished thesis (M.Sc), Michigan State University

[12] Zaidi, S. 2010, “Failure Diagnosis and Prognosis of Electrical Machines”. Unpublished Thesis (PhD), Michigan State University